SLAC-PUB-502
September 1968
(EXP)

ELECTROMAGNETIC INTERACTIONS: LOW q^2 ELECTRODYNAMICS; ELASTIC AND INELASTIC ELECTRON (AND MUON) SCATTERING*

W.K.H. PANOFSKY

Stanford Linear Accelerator Center
Stanford University, Stanford, California

(Presented at XIVth International Conference on High Energy Physics, August 28 to September 5, 1968, Vienna.)

*Work supported by the U.S. Atomic Energy Commission.

ELECTROMAGNETIC INTERACTIONS

I. Electrodynamics at Low Momentum Transfer

In discussing electromagnetic processes at high energies it is customary to start examining the validity of electrodynamics at high momentum transfers.

We will depart from tradition by dividing the subject into a discussion of quantum electrodynamics at low momentum transfers with high precision and high momentum transfers at low precision. I will deal with the first subject while other speakers will deal with the second. The justification for this otherwise illogical procedure is that high momentum transfer QED from the experimental point of view happens to overlap with experiments on the photoproduction of vector mesons and their leptonic decays, and also that storage ring work on high momentum transfer electrodynamics coincides with those experiments which again relate primarily to vector meson production processes; both of these subjects fall into the province of other rapporteurs. Another reason permitting splitting a discussion of the validity of QED into these two regions is the fact that the relation between low and high energy momentum transfer processes is highly model-dependent,should a meaningful deviation be found. At this time there is no reason for confidence in a particular model of a deviation, nor is there any persuasive evidence for the existence of any deviation, either from high q^2 or low q^2 experiments.

Low momentum transfer quantum electrodynamics is in a somewhat confusing state. On the one hand one problem which has plagued physicists for the last years, namely the problem relating to consistency among different methods of determining the fine structure constant, has probably gone away. On the other hand, the discrepancy of the value of the Lamb Shift with theory has persisted and new discrepancies in the values of the g factor of the muon and electron seem to have appeared. I believe however, it is also fair to say that none of these discrepancies are such that they may not be either experimental in nature, or may be the result of subtle points having been missed in analysis.

To discuss these questions let me first make reference to the spectrum of the hydrogen atom (Fig. 1). In past years the hydrogen fine structure discrepancy has been identified by plotting values of

$$\alpha^{-1} - 137$$

which appeared to cluster near two values, one being .036, and the other .039. Although only few experiments have been reported to this conference which bear on this question I would like to discuss the complete picture in order to provide some context.

The hyperfine structure of the ground state of hydrogen gives the experimental value [1] of

$$\nu^{H}_{HFS} = 1420.405\ldots\text{MHz}$$

as measured by the hydrogen maser. The precision is beyond anything of interest here. The problem is mainly a theoretical one, namely how to take the nucleon structure into account. If one makes a purely static calculation [2] of nucleon structure, the value of the fine structure constant becomes

$$\alpha^{-1} = 137.0359$$

accurate to about one part per million. Although I am plotting this particular value on the summary sheet (Fig. 2) of values of the fine structure constant, there is little question that a static calculation will probably overestimate the effect of finite nucleon size. The reason is that as the electron moves around the nucleon the polarization of the nucleon will vary correspondingly and therefore the effective finite size effect might be smaller. This effect has been estimated by Drell and Sullivan [3] and might give an additional correction in α of the order of five parts per million. It is this uncertain theoretical picture which has led people in the past not to take the HFS value of Alpha too seriously, although no rational reason has been presented why the error should be larger than that estimated.

A shift has occurred during the last year in the measurement of the hyperfine structure of muonium. Amato, _et al._, [4] have reported measurements of the hyperfine structure of muonium at very low magnetic field (10^{-2} gauss) in which the Zeeman-splitting has not been resolved. In a paper submitted to this conference they quote:

$$\gamma^{\mu}_{HFS} = 4463.25 \pm .06 \text{ MHz}$$

which is slightly higher than the values quoted earlier [5] at higher magnetic fields. To go from these measurements to a value of the fine structure constant we need the measurement of the ratio of the muon moment to the proton moment as measured by the ratio of precession rates; this ratio is known to about 12 parts per million, and the correction due to Ruderman [6] which corrects for the fact that the proton and the muon find themselves in different chemical fields when undergoing such precession. Applying these auxiliary considerations one obtains

$$\alpha^{-1} = 137.0369 \pm .0013 \quad .$$

Although the use of muonium and also positronium is attractive to avoid the complications of finite nucleon structure in hyperfine structure, the muonium measurements are marred by such auxiliary considerations while the positronium measurements and also the calculation of positronium fine structure have as yet not reached sufficient accuracy.

Let us now return to the proton: The most direct measurement of the fine structure constant should presumably derive from measurement of the fine structure interval ($2p^{3/2} - 2p^{1/2}$) as shown in Fig. 1. Historically the most accurate measurement was that of Lamb and collaborators (Dayhoff, et al, [7]) which measured the $2p^{3/2} - 2s^{1/2}$ interval and added to this the value of the Lamb Shift interval ($2s^{1/2} - 2p^{1/2}$). This combination gave a value of $\alpha^{-1} - 137$ slightly lower than .039 which had been extensively quoted in the literature and which is plotted in Fig. 2. However, two recent measurements have changed the situation: A direct measurement [8] of the fine structure separation has been made by determining precisely the magnetic field required to lead to crossing of the $2p^{3/2}$ and the $2p^{1/2}$ levels. This measurement has given a value of

$$\alpha^{-1} = 137.0353 \pm .0008 \quad .$$

Although this may appear to be a more straightforward approach than that of Dayhoff, et al., [7] one still should note that the error quoted requires confidence in locating the line to one part in 2,000 of its width; for this one has to rely on complete theoretical understanding of line shape. Recently another measurement [9] has been made of the $2p^{3/2} - 2s^{1/2}$ interval, which when combined with the experimental Lamb Shift interval gives a value of

$$\alpha^{-1} = 137.0359 \pm .0007$$

for the inverse fine structure constant.

Finally, we have the new result obtained with cryogenic techniques which gives new precision to the ratio of Planck's

Constant to the electronic charge. This work by Parker, et al., [10] used the precision determination of the voltage generated in a Josephson Junction when irradiated at a fixed microwave frequency. This voltage appears to be related to the frequency in the cavity by the equation

$$2eV = h\nu$$

from which the fine structure constant can be determined by the equation

$$\alpha^{-1} = \left(\frac{mc}{2Ry_\infty \hbar}\right)^{1/2} \left[\frac{c}{4\ Ry_\infty} \left(\frac{\mu_p}{\mu_o}\right)\left(\frac{1}{\gamma_p}\right)\left(\frac{2e}{h}\right)\right]^{1/2}$$

where Ry_∞ is the value of Rydberg constant at infinite mass measured in inverse centimeters and where γ_p is the gyromagnetic ratio of the proton, while (μ_p/μ_o) is the value of the proton magnetic moment measured in Bohr magnetons. These auxiliary constants are known to sufficient precision that Parker et al., could quote a value of

$$\alpha^{-1} = 137.0359 \pm .0004 \quad .$$

The question of whether the theory of the Josephson Junction is really sufficiently clean to permit confidence in this measurement has recently been answered experimentally to almost complete satisfaction by a series of remarkable measurements by John Clarke [11]. He demonstrated that the Josephson voltage steps are independent of the nature of the materials used to about one part in 10^8.

All these experimental values when plotted on Fig. 2 suggest strongly that now all measurements of $\alpha^{-1} - 137$, other than the early ones of Dayhoff, _et al_. [7] , cluster about .036, and that the new muonium measurements reported to this conference appear to join the crowd.

Thus all appears to be well excepting for the fact that the measurements of the Lamb Shift itself (which affect the determination of α only in a minor way through addition to the partial fine structure interval $2p^{3/2} - 2s^{1/2}$) continue to fail to agree with theory. The two independent measurements, one the direct measurement of the separation due to Lamb and co-workers [12], and the other by the level crossing method of Robiscoe, _et al_., [13] are now in agreement with one another to within about two standard deviations but are in disagreement with theory by more than four standard deviations; most of the estimate of probable error rests on uncertainty of theory rather than experiment.

Let me now go on to the g-factors. During the preceding conferences (Stanford and Heidelberg) the CERN group of Bailey, _et al_., announced progress of their measurements on the g-2 value of the muon using their 1.5 GeV weak-focusing muon ring. I assume that the disposition of the experiment is well-known and will not repeat it here. Out of these measurements a discrepancy between theory and experiment had apparently emerged. At this conference Bailey, _et al_., [14] announce a value of

$$(g-2)/2 = (116614 \pm 31) \times 10^{-8}$$

for the muon anomaly which compares to a quoted theoretical value of

$$(g-2)/2 = (116560) \times 10^{-8}$$

if QED is assumed to be valid to smallest distances, and where estimates of strong interaction loops and the effect of a possible intermediate boson have been included. The deviation is thus reduced to $(54 \pm 31) \times 10^{-8}$ in $(g-2)/2$ which may no longer deserve to be called a discrepancy.

There are both theoretical and experimental sources of the uncertainty in the gyromagnetic anomaly of the muon. Even the contribution from pure quantum electrodynamics to the anomaly (for which no uncertainty is discussed by the authors) still has an outstanding contribution to the α^3 term which has not been calculated as yet. The hadronic contribution to the anomaly has been calculated [15] using the rho meson width and height from the earlier Novosibirsk experiments [16] and inferring the omega and phi contributions from SU(3). More recent data on the ρ vector meson are now available from Novosibirsk and directly measured widths and amplitudes of the ρ and other vector mesons from the Orsay colliding beam experiments are reported at this conference. For this reason the theoretical correction to the anomaly due to hadronic contributions might well shift by a few parts in 10^8, but this point can be cleared up with the new data. The weak interaction correction is very small and therefore its uncertainty appears not to be significant.

However, it should be noted that this calculation assumes an intermediate boson without an anomalous magnetic moment to moderate the Fermi interaction; the correction would increase linearly with a possible anomalous moment of the W; moreover the calculation requires cut-off procedures. Considering all the circumstances one might conclude that a presumed theoretical uncertainty of $\pm 10 \times 10^{-8}$ is not overly generous.

The group of Bailey, et al., has carried out diligent searches for sources of error in their experiment which might account for the deviation. The mean life of muons trapped in the ring appears to lengthen with trapping time and approaches the theoretical value at large times, thus indicating some continued muon loss; this loss is probably caused by imperfections in the magnetic field. This, combined with the fact that the measurement of mean magnetic field as seen by the trapped muons rests on observation of the cyclotron frequency of the initially trapped bunches, gives rise to speculations that possibly the mean field seen during the entire muon history and that seen by the early bunches may not be the same. This effect has been studied experimentally by using different time intervals for observation of the bunch rotation frequency, and consistent results were obtained; however, there is an unexplained loss of particles between the time intervals chosen. In addition many checks using variable aperture stops have given consistent results with the orbit population calculated by Monte Carlo methods. The shift in mean orbit radius required to remove the deviation is in excess of permissible limits. The reason for the reduction of the deviation relative to the result reported earlier is attributed to the fact that the data interval used in the fitting of the precession for the preliminary result started at a time t_1, which was unfortunately atypical. In the measurement reported here a variety of starting times were used; a systematic dependence on the starting time t_1 was discovered and has been corrected for.

Discussions of a new version of this experiment are under way at CERN and in the U.S., since a possible deviation in the measurement of this important quantity clearly needs confirmation.

The situation concerning the electron g-factor is no better. Rich [17] has recently recalculated the old measurements of Crane and collaborators and has uncovered corrections originally overlooked. The measurement can be quoted by stating that the α^3/π^3 term appears to have a coefficient

$$-(6.5 \pm 2.5)$$

as compared to the theoretical estimate of .15 . Note that this discrepancy*, if any is in the opposite direction of that of the g-factor of the muon. As an experimentalist one has, of course, not the greatest confidence in such recently

* $[(g-2)/2]_{electron;experimental} = (115955.7 \pm 3.0) \times 10^{-8}$

$[(g-2)/2]_{theoretical;137-\alpha^{-1}=.036} = (115964.1 \pm .3) \times 10^{-8}$

resurrected corrections to an old measurement and one hopes for a new determination. Experiments using cryogenic and other techniques are under way towards that end in several laboratories.

This is the situation on low momentum transfer electrodynamics. Some clarity has been added in one corner but possible problems have emerged in others. I will now proceed in the rest of the talk to sweep all these problems under the rug and assume that quantum electrodynamics is an exact science.

II. Elastic Electron-nucleon and Muon-nucleon Scattering

In addition to assuming the validity of quantum-electrodynamics over the full range of parameters covered, all analyses of elastic and inelastic scattering experiments continue to assume single photon absorption only. This assumption can be tested by comparing electron and positron scattering cross sections, by observing the polarization of the recoil nucleon, and by observing deviations from a linear "Rosenbluth" plot. The recent work of Mar *et al.*, [18] has extended the positron-electron comparison to $q^2 = 5(\mathrm{GeV}/c)^2$ without any evidence for a deviation from equality of the cross sections for elastic and some inelastic scattering from the proton.

The measurements give limits on the real part of the two photon exchange amplitude rela[illegible] to the one photon amplitude of the order of one per[illegible]. No further new evidence on the two photon amplitudes has been developed recently; none of the numerous "Rosenbluth" plots involved in the elastic and inelastic scattering experiments reported below exhibit deviation from the straight line relationship of the cross section with $\tan^2(\frac{\theta}{2})$ where θ is the scattering angle.

Relatively little new experimental information has been submitted to this conference on elastic electron-nucleon scattering. You may recall from an earlier conference that at SLAC [19], spectrometer experiments have extended measurements on electron proton scattering to four-momentum transfers of $q^2 = 25(\text{GeV/c})^2$, and that these data continued to fit reasonably well the so-called "dipole" formula for the form factor, although this fit exhibits some deviations when viewed in detail. Earlier data from DESY showed agreement with the so called "scaling law"

$$G_{Ep}(q^2) = \frac{G_{Mp}(q^2)}{\mu_p} = \frac{G_{Mn}(q^2)}{\mu_n} \simeq \frac{1}{(1+q^2/.71)^2} .$$

Recent precision measurements [20] using the external beam of the Bonn 2.5 GeV electron synchrotron have given the first possibly statistically significant indication that the scaling law may be violated. The Bonn data cover a range to $2(\text{GeV/c})^2$ as shown in Fig. 3 and can be fitted by an equation of the form

$$G_{Ep}(q^2) = G_{Mp}(q^2)\left[1-(0.063 \pm 0.018)q^2\right]/\mu_p$$

Considering the difficulties of these measurements the authors do not claim that this deviation is necessarily significant.

The data on the electric form factors of the neutron remain in an extremely unsatisfactory state but are compatible with being close to zero everywhere; however the interaction between electrons and thermal neutrons leads to a non-vanishing derivative of the electric form factor of the neutron at $q^2 = 0$.

The slope of the variation of $G_{En}(q^2)$ with q^2 is no longer in disagreement with the low ($q^2 < 0.2(\mathrm{GeV}/c)^2$) measurements [21]. This is partially due to an upward shift of these measurements of $G_{En}(q^2)$ originating from elastic scattering on the deuteron at low q^2 and from improved dispersion calculations presented at this conference [22]. The situation is shown in Fig. 4. There is some new experimental material at higher values of q^2: Recent measurements are reported at this conference by Galster et al., [23] on deuteron elastic scattering using an electron deuteron coincidence technique. The result places a new upper limit on the value of G_{En}; the results are $G_{En} = 0.02 \pm 0.05$ at $q^2 = 0.27(\mathrm{GeV}/c)^2$ and $G_{En} = 0.06 \pm 0.06$ at $q^2 = 0.4(\mathrm{GeV}/c)^2$. The limit in the total range $0 < q^2 < 3(\mathrm{GeV}/c)^2$ remains $|G_{En}|^2 < 0.3$ which is not sufficiently stringent for useful analysis. Extending measurements of the electric form factor of the proton, let alone the neutron, to high momentum transfers will be attempted but progress is very difficult since de facto such a measurement involves subtraction of cross sections measured under dissimilar kinematic conditions with only a small residue remaining.

Theoretical interpretation of the elastic scattering data will be discussed in another session. Let me only say here that not too satisfactory a picture has emerged. Attempts have been continued to fit the measured form factors with poles in the time-like region of momentum transfer but such fits require both large finite widths as well as pole locations at energies where no physical particles are observed.

Several attempts have been made to relate electron-proton scattering to proton-proton scattering data, as first suggested by Wu and Yang [24]. Experimentally we can show the correspondence by plotting both the ratio $(\frac{d\sigma}{dt})/(\frac{d\sigma}{dt})_{t=o}$ for proton-proton scattering as well as $G^4_{Mp}(t)/G^4_{Mp}(0)$ against $t = -q^2$; this is done in Fig. 5; this plot leads to the striking inference [25] that as $s \to \infty$ the relation

$$(\frac{d\sigma}{dt})_{p-p} = (\frac{d\sigma}{dt})_{p-p;t=o}\ G^4_{Mp}(t)$$

might become exact.

The disadvantage of this simple conjecture is that there is no experimental proof for its correctness; the advantage is that it leaves no free parameters so that predictions result for proton-proton scattering at energies accessible to the Serpukhov accelerator. More specific discussions on interpreting the correspondence between e-p and p-p scattering and other attempts to account for the q^{-4} behaviour of the form factor at large q^2 are contained in the theoretical sessions.

Muon-proton elastic scattering data on hydrogen presented at this conference from Brookhaven [26] have not demonstrated any difference between electron and muon scattering; the highest momentum transfer reached is $q^2 = 0.9(\text{GeV/c})^2$. The inelastic muon scattering experiment from SLAC [27] reported at this conference also shows equality of electron and muon properties within experimental error.

The experiment of Lederman et al.,[26] used a combined spark-chamber and range-chamber technique in a purified muon beam with pion contamination less than one part per million; beam momenta ranged from 6 GeV/c to 17 GeV/c with detection efficiency of about 30% at best. The results demonstrate

a) equality of μ^- and μ^+ scattering;

b) Straight - line behaviour on "Rosenbluth" plots.

c) Equality of electron and muon scattering with the exception of an unexplained normalization error of 8%.

Fig. 6 shows the resultant fit of the μ-p data expressed as a form factor, assuming validity of the "scaling law" $G_E = G_M/\mu$.

Another experiment dealing with the question of equality of muon and electron interactions was reported by Russell et al [28] on the observation of muon "tridents", that is to say the process of muon pair production by incident muons. Since two of the final muons have identical charges, the cross section is sensitive to the statistics obeyed by the muon. Although the reaction was clearly observed for the first time, the experiment was not sufficiently sensitive to differentiate between Fermi and Bose Statistics.

To summarize we find that all evidence currently available relating to the electromagnetic interactions of leptons does not reveal any deviation from muon-electron equality.

III. Inelastic Electron Scattering on the Nucleon

Possibly the most important experiments in the field of high energy electrodynamics reported in this conference are in the field of inelastic electron scattering. Part of this field is just beginning to be exploited and therefore the results reported here are frequently only indicative and their full power will have to be demonstrated later.

Inelastic electron scattering gives results in the following areas:

(a) Test of T violation

(b) Examination of the pion electromagnetic form factor

(c) The form factors of specific resonant states and extrapolation of inelastic electron scattering to zero momentum transfer, yielding the total photon absorption cross sections

(d) Examination of the excitation of the nucleon into the continuum.

Let me discuss the relevant information on these four topics in the order given, although information on each topic frequently results from the same experiments.

(a) Tests of T-violation

After the discovery of CP violation in neutral kaon decay, speculations by T. D. Lee and collaborators indicated the possibility that electromagnetic interactions involving hadrons might also exhibit T-violations. The likelihood of such predictions corresponding to reality has undergone several fluctuations as further information on such questions as the η decay asymmetry, the electric dipole moment of the neutron, and other relevant parameters has become available.

It was suggested specifically by Christ and Lee [29] that a T-violating asymmetry predicted in interactions of the kind:

$$(\vec{p} \times \vec{p}\,') \cdot \vec{\sigma}_p$$

might be detectable by inelastic electron scattering of electrons of initial momentum $\vec{p}$, final momentum $\vec{p}\,'$, scattering on protons of spin orientation $\vec{\sigma}_p$. It can be shown that such a term cannot be present in elastic scattering. However it can also be shown that should the data exhibit the asymmetry implied by such an interaction this can be taken as a proof of violation of T invariance only if the process can be described purely by one photon exchange. Therefore, should an asymmetry be found, the result should be checked with inelastic positron scattering. The choice of the specific excited state offers an additional complication: The most prominent state available to study by inelastic electron scattering is the $N^*(1238)$. However, since the isotopic spin of $N^*(1238)$ is 3/2, no asymmetry would be expected in inelastic scattering should the T violating interaction be an isotopic scalar. Therefore the most conclusive test on this question would be study of the asymmetry of inelastic scattering from $N^*(1512)$

which has isotopic spin 1/2. Experimental results on this question have been reported to this conference by Appel, et al., [30] using the CEA external electron beam. The polarized target used was a "doped" mixture of ethanol and water in which typical proton polarizations of about 24% were attained. Radiation damage to the target by the electron beam required frequent changes of target. This experiment is a very difficult one since statistics of observation of the asymmetry are diluted by scattering from the carbon component of the target, by the partial polarization of the protons and by the fact that the state under study is superimposed on a background of unknown character. The asymmetry in inelastic scattering is caused by interference between scattering of longitudinal and transverse virtual photons. The ratio between the effective longitudinal and transverse photon content involved in the scattering process is given by the well-known polarization factor $\varepsilon = 1/\{1+2[1+(E-E')^2/q^2]\tan^2\frac{\theta}{2}\}$ which is a purely kinematic quantity; here E and E' are the primary and secondary electron energies respectively; and $q^2 = 4EE'\sin^2\frac{\theta}{2}$ is the square of the four-momentum transfer; note that $q^2 = 0$ and thus $\varepsilon = 0$ for real (transverse) photons.

In general the differential cross section for inelastic scattering can be written as

$$\frac{d^2\sigma}{d\Omega dE'} = \Gamma_t\{\sigma_T + \varepsilon\sigma_s + [2\varepsilon(1+\varepsilon)]^{1/2}\frac{\vec{\sigma}_p\cdot(\vec{p}\times\vec{p}\,')}{|\vec{p}\times\vec{p}\,'|}\sigma_{Ts}\}$$

where $\Gamma_T(q^2, E'-E)$ is a purely kinematic factor given by $\frac{\alpha}{2\pi^2}\times\frac{E'}{E}\frac{K}{q^2}\frac{1}{1-\varepsilon}$ with $K = E-E'-q^2/2M = (M^{*2}-M^2)/2M$. Here K is the energy of the photon giving the same exitation M^* to the nucleon system as inelastic scattering of the electron. The quantiti σ_T and σ_s are the cross section per equivalent transverse and longitudinal photon respectively. The quantity σ_{Ts} is the effective cross section due to interference between transverse and longitudinal photon amplitudes. The degree of T violation can then be measured by a phase difference δ be - tween these two amplitudes. The asymmetry can then be shown to be

$$a = A \sin\delta = \frac{[2\varepsilon(1+\varepsilon)]^{1/2}}{\sigma_T + \varepsilon\sigma_s} \sigma_{Ts} \sin\delta$$

The relation of σ_{Ts} to σ_s and σ_T depends on the multipolarity of the transition which is well established for the 1238 and 1512 MeV resonances.

The authors give the following table for these results (Fig. 7). Clearly no evidence for T violation has been demonstrated and therefore there exists no incentive for the matching positron experiment. A similar experiment at higher energies and higher sensitivity is in preparation.

A second experiment examining T violation in electromagnetic scattering has been reported by Prepost et al., [31]. The experiment, following the suggestion of Kobsarev et al., [32] examines the polarization of recoil deuterons from elastic electron scattering. In contrast to the situation in the case of elastic (but not inelastic) scattering from spin 1/2 particles. elastic electron scattering from particles of spin 1 or greater can retain T-violating terms which do not vanish identically due to current conservation. The term in elastic electron-deuteron scattering corresponding to scattering by the quadrupole moment of the deuteron can interfere with a T-violating amplitude to give polarization to the deuteron; at the same time the square of the T-violating amplitude contributes to the elastic scattering cross section itself. An upper limit on the maximum polarization can then be estimated by ascribing the difference between the most recent measurements [33] of the elastic e-D scattering and the Born approximation calculation entirely to a T-violating term; this limit corresponds to a value of 0.34 for the polarization.

The experiment was carried out by analyzing deuterons recoiling from scattering by 1 GeV electrons using a magnetic spectrometer combined with time-of-flight identification. The identified deuterons were analyzed for right-left asymmetry by a carbon scatterer. The observed polarization was 0.070±0.083 which is well below the maximum value quoted above. Unfortunately it is difficult to relate this null result to the T-violation experiment using inelastic electron-proton scattering referred to above since the estimate of the maximum possible polarization in itself may be too large, quite apart from the question whether T-invariance violation may occur.

(b) The Pion Form Factor

Two methods for direct measurement of the pion form factor by electromagnetic means have been applied previously. One of the methods involves inelastic electron scattering; somewhat more sensitive measurements have been reported at this conference [34]. Inelastic electron scattering is observed under kinematic conditions where the pion pole diagram of low energy photoproduction plays a dominant role in the cross section. This diagram involves the direct absorption of the virtual photon by the emitted pion and therefore the resultant cross section should be sensitive to the pion form factor. Since this diagram cannot be separated from the other production amplitudes in a gauge invariant manner, isolation of the pion form factor demands the study of the sensitivity of a complete production model to the value of this form factor. Earlier experiments of this type have been carried out by Akerlof et al., [35]. The new data of Mistretta et al. [34] are shown in Fig. 8 . This figure shows the measurements compared to a simple ρ dominance calculation as well as to the more complete dispersion calculations of Zagury [36] in which the pion form factor is introduced as a free parameter. Both experiments can be fitted with a pion form factor equal to that of the proton but the data are also compatible with a simple ρ-vector dominance model. Considering that the RMS proton radius is 0.8 F while a ρ-vector dominance propagator as a form factor would give a radius of $\sqrt{6}/m_\rho = 0.63$ F, these measurements leave considerable uncertainty in the pion electromagnetic radius. The second approach to obtaining the electromagnetic pion form factor by observation of the interference term between Coloumb and nuclear scattering in pion helium scattering has thus far failed to give results which are quantitatively useful. Earlier work on this subject by M. M. Block and collaborators has yielded limits of error too wide to be significant; current work now in progress at LRL by Crowe [37] and collaborators appears to give a pion radius larger than 2 Fermis, but uncertainties in the theoretical analysis of the nuclear scattering makes this result not convincing.

Another experiment bearing on pion form factors but not using electron scattering is the study of Dalitz pairs from the π^- capture reactions at rest [38]

$$\pi^- + p \rightarrow n + \pi^0$$
$$\quad\quad\quad\quad\quad \hookrightarrow e^+ + e^- + \gamma$$

$$\pi^- + p \rightarrow n + \gamma$$
$$\quad\quad\quad\quad\quad \hookrightarrow e^+ + e^-$$

Previously the study of these processes has been used as tests of QED. Since the q^2 of specific QED tests has now reached limits well above those involved in these reactions, the pion capture processes can instead be used as pion form factor experiments . The point is of course that the Dalitz pair represents a finite mass photon coupled to the pion. The previous experiments have been bubble chamber experiments; this experiment used Sodium Iodide for measuring the Dalitz pairs and plastic scintillators for triggering; a lead plate spark chamber was used to detect the γ ray in the first reaction. About 2×10^4 events were taken. The result expressed as a form factor $F = 1 + xq^2/m_\pi^2$ gives $x = 0.01 \pm 0.11$ in contradiction to the old bubble chamber result -0.24 ± 0.16 .

The theoretical value of the neutral pion form factor gives a non-zero result if the pion decays into a γ ray and a vector meson* which then decays into a virtual γ ray. The resulting theoretical value is small (of the order of $x \approx 0.04$).

(c) Form Factors of Resonant States

Inelastic scattering leading to resonant states has been studied since 1958 and an increasing body of evidence has been accumulating on the subject.

Before introducing the new information available, let me briefly review the general formalism applying to the problem. According to a general theorem of Bjorken the differential inelastic cross section can be written as

$$\frac{d^2\sigma}{dq^2 d\nu} = \frac{E'}{E}\,\frac{4\pi\alpha^2}{q^4}\left[\cos^2\frac{\theta}{2}\,W_2(q^2,\nu)+2\sin^2\frac{\theta}{2}\,W_1(q^2,\nu)\right]$$

where $\nu = E - E'$, and where the W's define the nucleon properties. This form is equivalent to the equation used previously (with the T-violating term omitted), which shows more clearly how inelastic electron and muon scattering (virtual photo-production) relates to real photo-processes:

$$\frac{d^2\sigma}{d\Omega dE'} = \frac{E'}{E}\,\frac{\alpha}{2\pi^2}\,\frac{K}{q^2}\,\frac{1}{1-\varepsilon}(\sigma_T+\varepsilon\sigma_S) = \Gamma_T(\sigma_T+\varepsilon\sigma_S) \quad ;$$

* The decay vertex for a neutral pion going directly into a γ-ray and an electron-positron pair vanishes identically by C-conservation.

all quantities have been defined previously. The quantity σ_T is related to the photoproduction cross section σ_γ by the relation $\sigma_T(q^2 \to 0) = \sigma_\gamma$ while $\sigma_s \to 0$ as $q^2 \to 0$. These relations show how in effect inelastic electron scattering is an "off the energy shell" extension of photoproduction. Extrapolation to $q^2 = 0$ of electro-production cross sections at small electron scattering angles (after radiative corrections) is expected to give an independent, and probably highly accurate, measurement of the total hadronic photo-absorption cross section as a function of photon energy; other experimental methods for determining this quantity are discussed in another session.

The most extensive data are, of course, those relating to $N^*(1238)$, although much information is also being gathered on the 1520, 1680 and 1920 MeV resonances. Comparison of the data with specific models demands separation of the longitudinal and transverse cross sections by studying the experimental data as a function of the polarization parameter ε. Although qualitative data on this separation (generally indicating that the longitudinal element is small) have been obtained previously for several resonances at DESY, quantitative data are available for $N^*(1238)$ only.

The separation between longitudinal and transverse elements of $N^*(1238)$ has been accomplished up to $q^2 = 2.34$ GeV/c^2 in a contribution to this conference by Bartel, et al., [39]. They used the external beam of the DESY synchrotron together with a high resolution, magnetic spectrometer described previously. The angular range covered was 10° to 35°. Numerous curves were run as a function of the polarization parameter ε

defined previously. Transverse cross sections are in agreement with earlier work. The longitudinal cross sections are shown in Fig. 9, combined with the work of Brasse et al., carried out using the internal beam at DESY, and with the earlier work at Stanford. It is noted that the lower q^2 cross sections are in agreement with the earlier Stanford work of Lynch, et al., [40] while the longitudinal cross sections at values of q^2 larger than 0.7 GeV/c^2 are compatible with being zero. It is interesting to note that oscillatory behaviour of the longitudinal element has been predicted by the model of Walecka which is reported at a different session. However, experimental data, bearing on the longitudinal-transverse separation, resulting from a combination of work from different laboratories should be viewed with caution.

New high energy data have been presented to this conference from SLAC by Bloom et al., [41] and from the internal DESY beam by Albrecht et al, [42]; the new measurements have not as yet been extended over a sufficient range of parameters to permit separation of longitudinal and transverse elements.

In order to obtain meaningful cross sections considerable effort has to be devoted to carrying out radiative corrections in an exact quantitative manner. This can only be done consistently by a numerical method applied to the cross sections themselves since the measurements at each value of incident electron energy E and scattered energy E' contain radiative contributions from the entire kinematically accessible region which can feed E' from E at a given scattering angle. Specifically if we consider the situation at a given scattering angle θ as shown in Fig. 10 , then the cross section from the entire shaded triangular region contained between the kinematic point E, E' of interest and the kinematic line corresponding to elastic scattering can contribute to the observed cross section. Complete unfolding of the radiative corrections therefore demand in principle a complete set of measurements in the shaded triangular region in Fig. 10. An approximation to such a program has been carried out by the SLAC group using the methods of Mo and Tsai [43] at a production angle of 6° by interpolating among measurements made at four primary energy values between 7 and 16 GeV as shown in Fig. 11.

Figure 12 shows an inelastic spectrum taken at a primary energy of 7 GeV obtained before radiative correction and Fig. 13 shows the resultant spectrum after such a radiative correction has been applied. Figure 14 shows similar data taken at 16 GeV before correction and Fig. 15 shows the corrected data. The following features are evident from these measurements:

A. Three and possibly four resonant states are clearly distinguishable and their cross sections can be isolated using a fitting program which demonstrates that the amplitude of the excited states is quite insensitive to the polynominal order of the background assumed; the result is shown in Fig. 16.

B. The continuum excitation falls of much more slowly with momentum transfer than does the excitation of specific excited states. At higher angles data not presented here show that the spectra are almost totally dominated by the continuum.

Analysis of the amplitudes and widths of the states must be approached with caution, since in particular the background subtraction program may be sensitive to the assumption as to spectral shape. With this caveat, the cross sections for three of the states are shown in Fig. 17. Similar data at lower primary energy but much larger scattering angle (about 48°) are derived from the recent DESY work [42]

Some simple connections can be drawn:

A. It appears from the work at DESY [42] that the inelastic cross section near the $N^{*}(1238)$ resonance falls off more rapidly with q^2 then near the higher resonances; considering the uncertainties in background subtraction, this interesting result is in need of confirmation when applied to the form factors themselves.

B. From the SLAC data [41] it appears that for large q^2 the fall-off of the cross section matches that observed in elastic scattering; Figs. 18, 19 and 20 show this clearly for $N^{*}(1238)$, $N^{*}(1512)$ and $N^{*}(1688)$; theoretical curves are those discussed by Walecka at a different session. At low q^2 the "threshold behaviour" depends on the angular momentum of the state; e.g. for a magnetic dipole transition we should have simply

$$\sigma_T(q^2,K) = \sigma_\gamma(K)|\vec{q}|^2|G_{MV}(q)^2/G_{MV}(0)|^2$$

where $G_{MV}(q^2) = G_{Mp}(q^2) + G_{Mn}(q^2)$ is the isotopic vector form factor of the nucleon. Figure 21 shows a plot from the recent DESY work qualitatively verifying a relation of this type; agreement is fair. However, comparison of the excitation of the $N^*(1238)$ as observed at SLAC with the complete dispersion calculations of Adler [44] shows that the experimental cross sections are well above the theory. Fig. 22 shows the data from the DESY external beam experiment [39] for the cross section of $N^*(1238)$ as a function of q^2 . The authors express the q^2-dependence as a product of $|\vec{q}|^2$ times an "effective" form factor $G^*(q^2)$ which is plotted in comparison with the dipole formula. Some deviation is observed but the fit to the dispersion calculations of Gutbrod and Simon [45] is good.

All old and newly available data from the various laboratories relating to the four resonances have been collected and are plotted in Fig. 23. The quantity shown as a function of q^2 is $\Gamma_T^{-1}\, d^2\sigma/d\Omega dE'$ which should approach the photoproduction σ_γ as $q^2 \to 0$; this limit is also shown.

It has been speculated that the "Roper" resonance $N^*(1470)$ whose existence has been inferred from phase shift analysis of π-p scattering should be prominently excited by inelastic electron scattering. Neither the SLAC [41] nor the DESY [42] work has revealed its existence. A special search on a neutron (i.e. deuteron) target at CEA by Alberi et al., [46] likewise has given negative results; the photo cross section obtained by extrapolating the data to q^2=o is estimated to be less than 120 μb.

(d) Continuum Excitation

Possibly the most important implication of inelastic scattering which, however, rests on very incomplete data, relates to excitation of the continuum. Here detailed interpretation will have to await further data, but some general remaks can be made in terms of the W_1 and W_2 formalism discussed above.

For small angle θ the ratio of the contribution to the differential scattering cross section of the W_1 term to that of the W_2 is given by

$$\frac{\sigma_T}{\sigma_T + \sigma_s} \frac{(E-E')^2}{2EE'} \text{, where } \sigma_T \text{ and } \sigma_s$$

are the cross sections per transverse and longitudinal photon as defined previously.(For moderate inelasticity and high primary energies this term is small for the entire region $0<\sigma_T/\sigma_s< \infty$). From SLAC data the function $W_2(q^2,\nu)$ is plotted numerically against ν for various values of q^2 in Fig. 24, assuming W_1 to vanish. Note that the continuum cross sections appear to converge to a ν^{-1} behaviour for large inelasticity. This same data can be plotted in different parameterization: Fig. 25 shows the function

$$F(\omega) = [\nu W_2(q^2,\nu)]$$

plotted against the variable ν/q^2. Since, as mentioned above, the experimenters have as yet not been able to gather the necessary data for separating the transverse and longitudinal elements, the curve is plotted under the alternate assumptions of vanishing of either the transverse or the longitudinal cross sections. Two striking facts emerge from this parametrization:

1. At least qualtitatively, using the variable ν/q^2 leads to a fairly universal representation of the "deep" inelastic continuum covered so far.

2. The function plotted appears to approach a constant for large ν/q^2. The inelastic muon data reported by Zipf et al., [27] cover inelasticities up to an equivalent photon energy of 7 GeV and a range of $q^2 < 0.9$ $(\text{GeV/c})^2$. An optical spark chamber technique is used; the statistical accuracy is of course well below that of the electron data. Within this limited accuracy there is fair agreement in the region of overlap between the electrons and muons.

The qualitatively striking fact is that these cross sections for inelastic electron and muon scattering leading to the continuum are very large and decrease much more slowly with momentum transfer than the elastic scattering cross sections and the cross sections of the specific resonant states; in fact indications are that they decrease probably even slower than what would be predicted from a simple ρ-vector dominance propagator. Therefore theoretical speculations are focused on the possibility that these data might give evidence on the behaviour of point-like, charged structures within the nucleon.

Treating the proton by a non-relativistic point quark model, Godfrey has derived a sum rule for the integral $\int W_2(q^2,\nu)d\nu$. Evaluation of the integral over the SLAC data gives about 60% of the required amount. There is no visible quasi-elastic peak at a defined inelasticity $\nu = q^2/2m$ where m is some characteristic mass, but the apparent success of the parameterization of the cross sections in the variable ν/q^2 in addition to the large cross section itself is at least indicative that point-like interactions are becoming involved. Numerical evaluation of the sum rules is difficult since the integrals will converge only if the curves shown in Fig. 25 eventually decrease more rapidly with (ν/q^2) than over the region covered by present data.

I have only attempted to point out the qualitative features of the data; specific comparisons with models and sum-rules are discussed in the theoretical sessions. However, a great deal more fundamental experimental material must be developed in this field before a clear picture can emerge.

REFERENCES

1. S. B. Crampton, D. Kleppner and N. F. Ramsey, Phys.Rev. Letters 11, 338 (1963); R. Beehler et al., Proc. IEEE 54, 301 (1966).

2. C. K. Iddings, Phys.Rev. 138, B 446 (1965).

3. S. D. Drell and J. D. Sullivan, Phys.Rev. 154, 1477 (1967).

4. J. J. Amato, P. Crane, V. W. Hughes, R. M. Mobley, J. E. Rothberg, G. zu Putlitz and P. A. Thompson, Vienna Conference 1968, Paper # 214.

5. W. E. Cleland, J. M. Bailey, M. Eckhouse, V. W. Hughes, R. M. Mobley, R. Prepost and J. E. Rothberg, Phys. Rev. Letters 13, 202 (1964).

6. M. A. Ruderman, Phys.Rev. Letters 17, 794 (1966).

7. E. S. Dayhoff, S. Triebwasser and W. E. Lamb, Jr., Phys. Rev. 89, 106 (1957).

8. H. Metcalf, J. R. Brandenberger and J. C. Baird, Phys.Rev. Letters 21, 169 (1968).

9. Kaufman, Leventhal and Lea, (to be published).

10. W. H. Parker , B. N. Taylor and D. N. Langenberg, Phys.Rev. Letters 18, 287 (1967).

11. J. C. Clarke, (to be published). The accuracy claimed has been reduced from 10^{-11} to 10^{-8} in a private communication.

12. S. Triebwasser, E. S. Dayhoff and W. E. Lamb, Jr., Phys.Rev. 89, 98 (1953).

13. R. T. Robiscoe, Phys.Rev. 168, 4 (1968) and subsequent communications.

14. J. Bailey, W. Bartl., G. V. Bachman , R. Brown, F. Farley, H. Jöstlein, E. Picasso, and R. W. Williams, Vienna Conference, 1968, Paper # 405.

15. B. E. Lautrup and E. de Rafael, BNL 12567 (May 1968).

16. Proceedings of the Heidelberg Conference on Elementary Particles, Sept. 1967, p. 386.

17. A. Rich, Conference on Atomic Masses, University of Manitoba, Winnipeg, (Aug. 28 - Sept. 1, 1967), Proceedings pp. 383 ff., Phys.Rev. Letters 20, 967 (1968) and Erratum, Phys.Rev. Letters 21, 1221 (1968).

18. J. Mar, B. Barish, J. Pine, D. H. Coward, H. de Staebler, Jr., J. Litt, A. Minton, R. E. Taylor and M. Breidenbach, Phys.Rev. Letters 21, 482 (1968).

19. D. H. Coward et al., Phys.Rev. Letters 20, 292 (1968).

20. Chr. Berger et al., Vienna Conference (1968), Paper # 516.

21. For a review of the experimental material, see:

    G. Weber, "Nuclear form factors below 6 GeV", Proceedings of the 1967 Symposium on Electron and Photon Interactions at High Energies, SLAC (Sept. 5-9, 1967); see pp. 70-71.

22. G. Höhler, R. Strauss and H. Wunder, Vienna Conference (1968), Paper # 233

23. S. Galster, G. Hartwig, H. Klein, J. Moritz, K. H. Schmidt, W. Schmidt-Parsefall, D. Wegener and J. Bleckwenn, Vienna Conference (1968), Paper # 492.

24. T. T. Wu and C. N. Yang, Phys.Rev. 137, B 708 (1965).

25. H. D. I. Abarbanel, S. D. Drell and F. J. Gilman, Phys. Rev. Letters 20, 280 (1968).

26. L. M. Ledermann, L. Camilleri, J. Christenson, M. Kramer, Y. Nagashima, T. Yamanouchi, Vienna Conference (1968), Paper # 264.

27. T. F. Zipf, J. L. Brown, H. Bryant, T. Braunstein, M. L. Perl, J. Pratt, W. T. Toner and W. L. Lakin, Vienna Conference (1968), Paper # 370.

28. J. J. Russell, R. Sah, M. J. Tannenbaum, W. E. Cleland, D. G. Ryan, D. G. Stairs, Vienna Conference (1968), Paper # 221.

29. N. Christ and T. D. Lee, Phys.Rev. Letters 139, B 1650 (1965).

30. J. A. Appel, J. Chen, J. Sanderson, G. Gladding, M. Goitein, K. Hanson, D. C. Imrie, R. Madaras, R. V. Pound, L. Price, Richard Wilson and J. Zajde, Vienna Conference, Paper # 483 ; also J. Chen, Thesis, Harvard University (1968).

31. R. Prepost, R. M. Simonds and B. H. Wiik, Report no. HEPL 566, Stanford University, Stanford, California, (June 1968), Vienna Conference (1968), Paper # 786.

32. I. Kobsarev, L. B. Olson and M. V. Terentyev, JETP Letters 2, 289 (1965); see also, V. M. Dubovik and A. A. Cheshkov, Soviet Physics JETP 24, 111 (1967); D. Schildknecht, DESY 66/30 (1966); V. M. Dubovik, E. P. Likhtman and A. A. Cheshkov, Soviet Physics JETP 25, 464 (1967).

33. R. E. Rand, R. F. Frosh, C. E. Littig, and M. R. Yearian, Phys.Rev. Letters 18, 469 (1967).

34. C. Mistretta, D. Imrie, J. A. Appel, R. Budnitz, L. Caroll, M. Goitein, K. Hanson and R. Wilson, Vienna Conference (1968), Paper # 489.

35. C. W. Akerlof, W. W. Ash, K. Berkelman, A. C. Liechtenstein, A. Romananskas and R. H. Siemon, Phys.Rev. 163, 1482 (1967).

36. N. Zagury, Phys.Rev. 150, 1406 (1966).

37. K. M. Crowe, Conference on Intermediate Energy Physics, Los Alamos, (June 19, 1968).

38. S. Devons, Nissim, C. Sabat, P. Nemethy, E. Di Capua, A. Lanzara, Vienna Conference (1968), Paper # 338.

39. W. Bartel, B. Dudelzak, H. Krehbiel, J. McElroy, W. Meyer-Berkhout, W. Schmidt, V. Walther and S. G. Weber, Vienna Conference (1968), Paper # 821.

40. H. L. Lynch, J. V. Allaby and D. M. Ritson, Phys.Rev. 164, 1635 (1967).

41. E. Bloom, D. H. Coward, H. De Staebler, J. Drees, J. Litt, G. Miller, L. W. Mo, R. E. Taylor, M. Breidenbach, J. I. Friedman, G. C. Hartman, H. W. Kendall and S. C. Loken, Vienna Conference (1968), Paper # 563

42. W. Albrecht, F. W. Brasse, H. Dorner, W. Flanger, K. Frank, E. Ganssauge, J. Gayler, H. Hultschig, J. May, Vienna Conference (1968), Paper # 313.

43. L. W. Mo and Y. S. Tsai, Report no. SLAC-PUB-380 (to be published in Rev.Mod.Phys.).

44. S. L. Adler, unpublished calculation.

45. F. Gutbrod and D. Simon, Nuovo Cimento 51 A, 602 (1967).

46. J. L. Alberi, J. A. Appel, R. J. Budnitz, J. Chen, J. R. Dunning, Jr., M. Goitein, K. Hanson, D. C. Imrie, C. A. Mistretta and R. Wilson, Vienna Conference (1968), Paper # 484.

LIST OF FIGURES

18. The cross section ratio $\sigma_{resonance}/\sigma_{elastic}$ for $N^{*}(1236)$.

19. The cross section ratio $\sigma_{resonance}/\sigma_{elastic}$ for $N^{*}(1525)$.

20. The cross section ratio $\sigma_{resonance}/\sigma_{elastic}$ for $N^{*}(1688)$.

21. Plot of $\sigma_T[G_{Mp}(0)/G_{Mp}(q^2)]^2$ in $|\vec{q}|^2$. The exponent of the observed power law is a measure of the transition multipolarity.

22. Plot of the "effective" form factor $G^{*}(q^2)$ for $N^{*}(1238)$ production.

23. Plots of $(d^2\sigma/d\Omega dE')/\Gamma_T$ for the first four resonances, compiling data reports from various laboratories.

24. Plot of $W_2(q^2,\nu)$ vs. q^2 for various values of $\nu = E - E'$.

25. Plot of $F(\omega) = \nu\, W_2(q^2,\nu)$, as a function of $\omega = \nu/q^2$.

INTERVALS IN MHz

NOT TO SCALE

ERRORS AS STANDARD DEVIATIONS (ASSUMED AS 1/3 OF LIMITS OF ERRORS WHERE QUOTED).

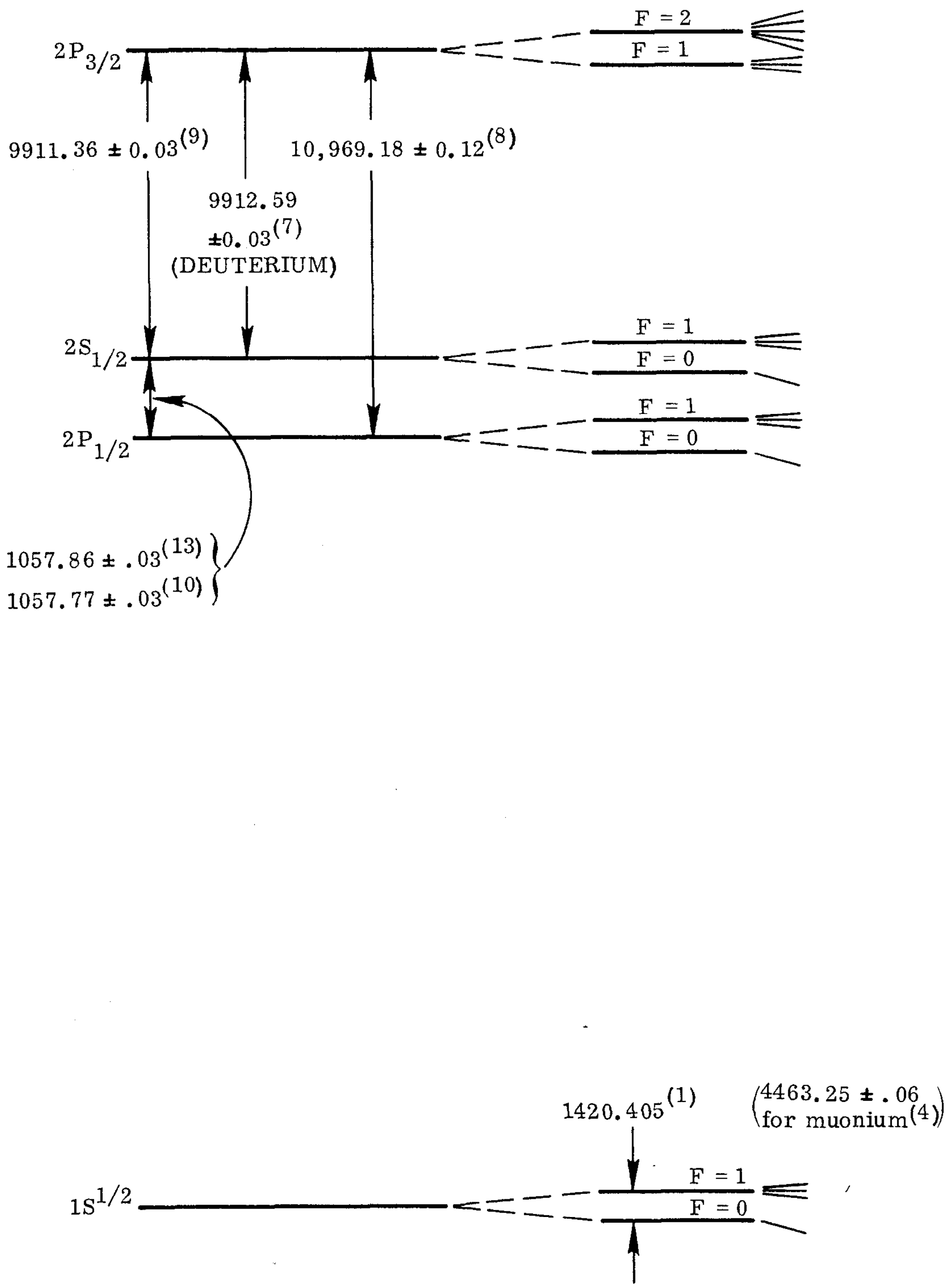

Fig. 1

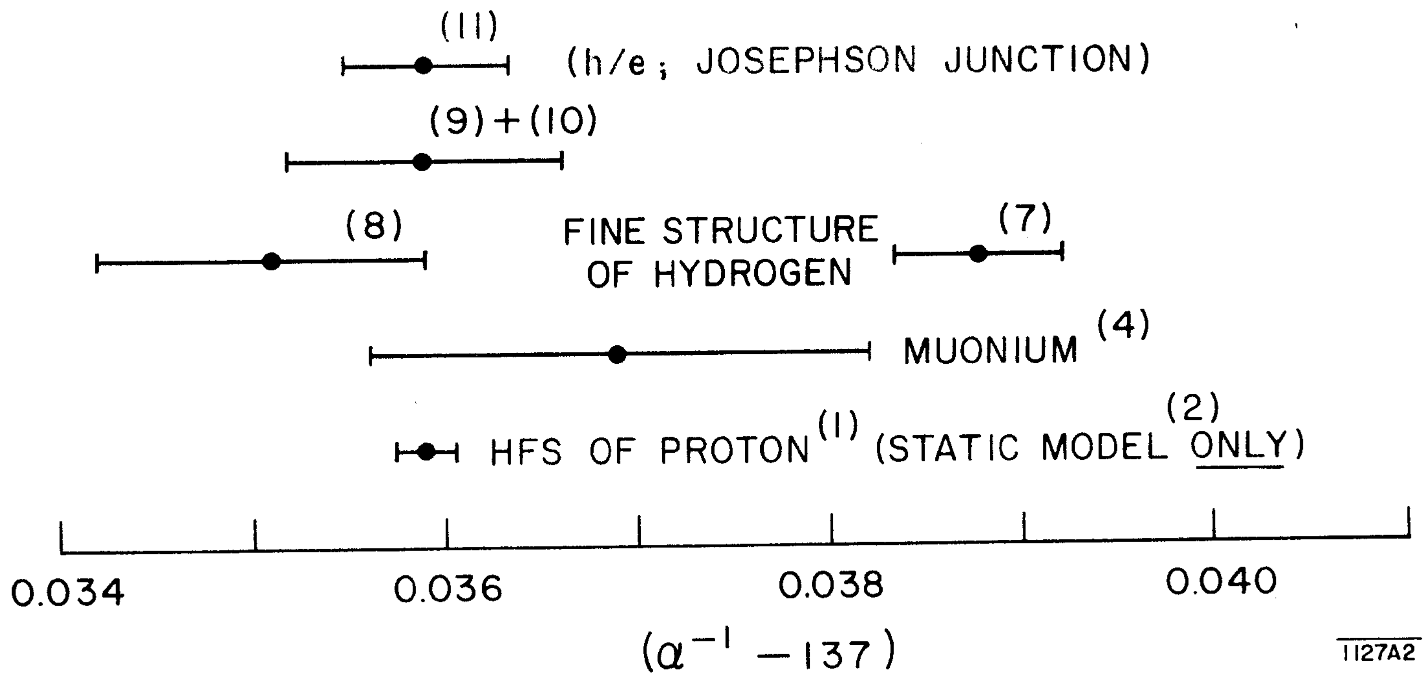

(11)
(h/e; JOSEPHSON JUNCTION)
(9) + (10)
(8)
FINE STRUCTURE
OF HYDROGEN
(7)
MUONIUM (4)
HFS OF PROTON (1) (STATIC MODEL ONLY) (2)
0.034
0.036
0.038
0.040
(α^{-1} − 137)
1127A2

Fig. 2

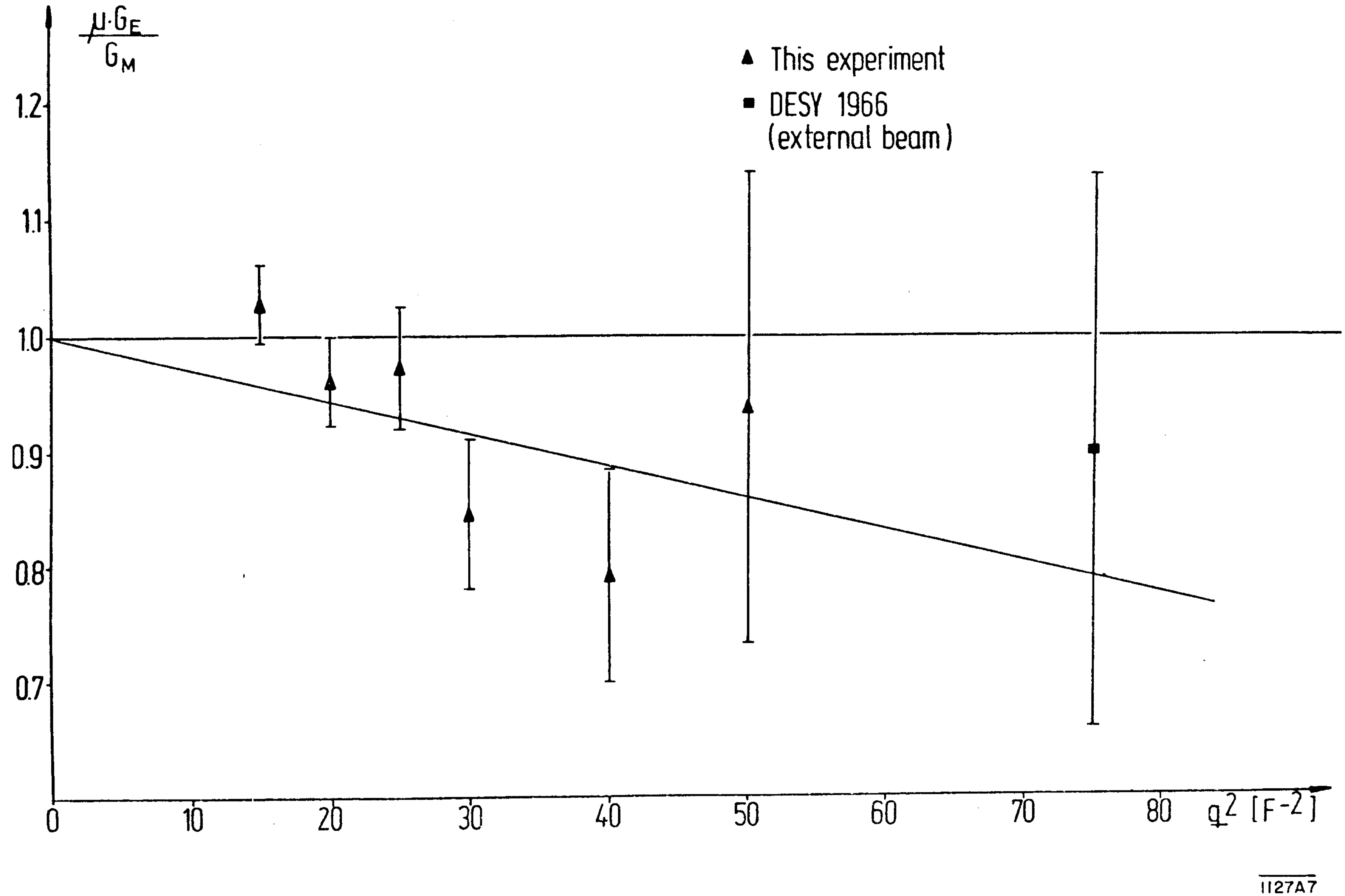
$\frac{\mu \cdot G_E}{G_M}$
This experiment
DESY 1966
(external beam)
1.2
1.1
1.0
0.9
0.8
0.7
0
10
20
30
40
50
60
70
80
q^2 [F^{-2}]
1127A7

Fig. 3

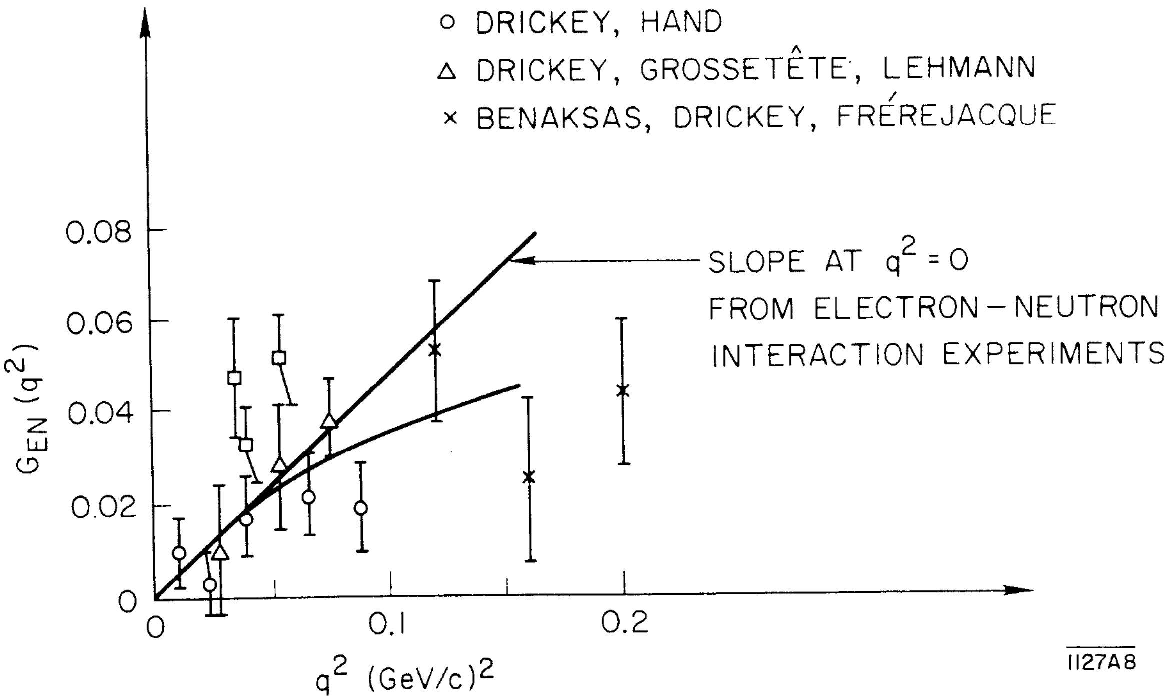
○ DRICKEY, HAND
△ DRICKEY, GROSSETÊTE, LEHMANN
× BENAKSAS, DRICKEY, FRÉREJACQUE
SLOPE AT $q^2 = 0$
FROM ELECTRON – NEUTRON
INTERACTION EXPERIMENTS
0.08
0.06
0.04
0.02
0
$G_{EN}(q^2)$
0
0.1
0.2
q^2 $(GeV/c)^2$
1127A8

Fig. 4

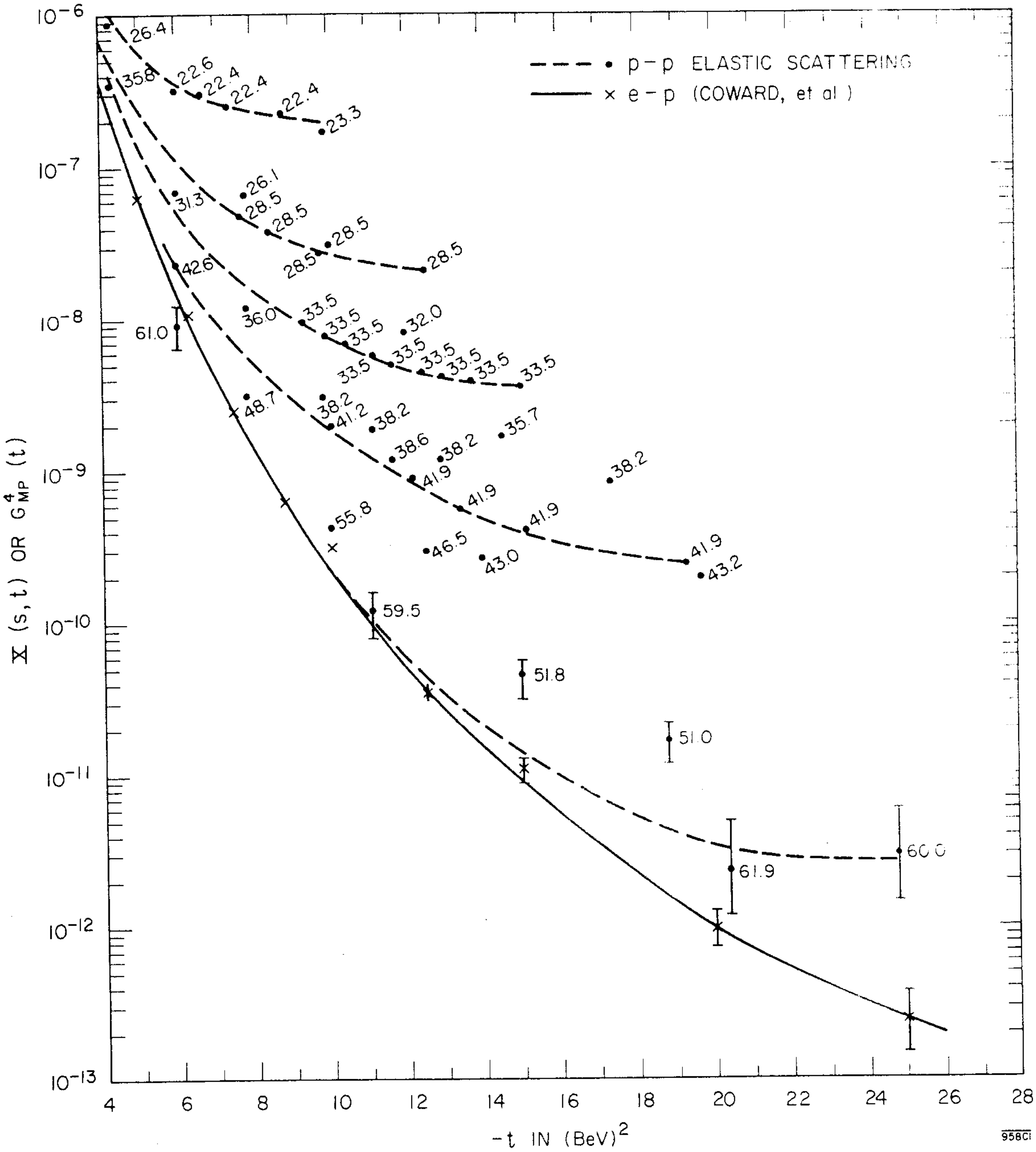

p−p ELASTIC SCATTERING
e−p (COWARD, et al)
X (s, t) OR G^4_{MP} (t)
−t IN (BeV)^2
958C1

Fig. 5

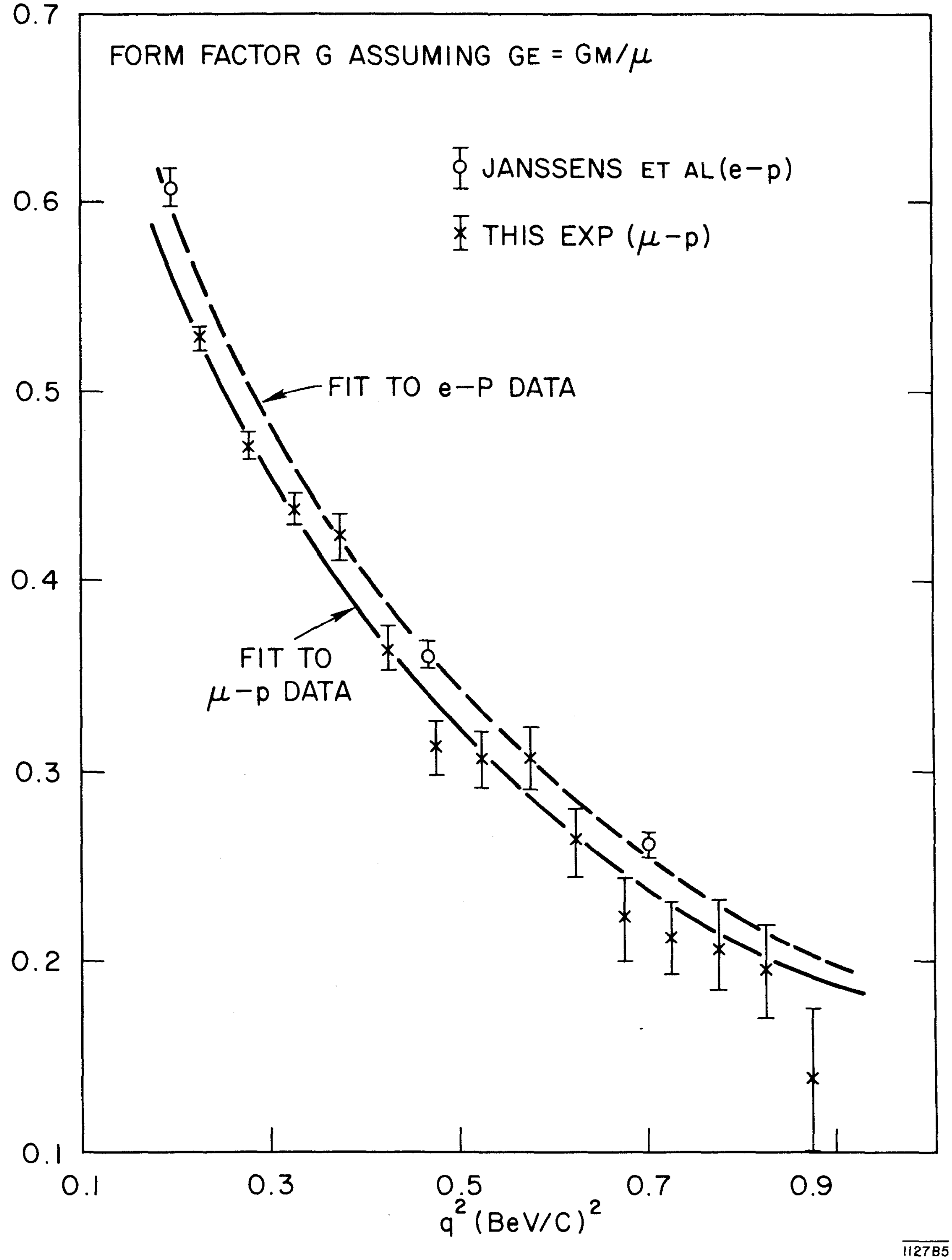
FORM FACTOR G ASSUMING GE = GM/μ
JANSSENS ET AL(e−p)
THIS EXP (μ−p)
FIT TO e−P DATA
FIT TO
μ−p DATA
0.7
0.6
0.5
0.4
0.3
0.2
0.1
0.1
0.3
0.5
0.7
0.9
q² (BeV/C)²
1127B5

Fig. 6

LIMITS ON THE T NONINVARIANCE PHASE δ AT W = 1238, 1512, 1470 and 1688 MeV

Resonance (MeV)	q^2 $(BeV/c)^2$	θ (Degrees)	A	(A)x(Correction Factor)	a/P	$\pm\Delta\epsilon/P$	δ	$\pm\Delta\delta$
1238	0.23	7.34	34%(1)	31%	3.5%	± 3.9%	6.5°	$\pm 7.2^\circ$
1512	0.52	7.59	39%(2)	36.5%	-2.4%	± 7.7%	-3.8°	$\pm 12.2^\circ$
1512	0.72	9.05°	39%(2)	36.9%	3.4%	± 4.4%	5.3°	$- 6.9^\circ$
1470	0.52	7.59	78%(3)	73%	-2.6%	±11.2%	-2.0°	$\pm 8.8^\circ$
1470	0.72	9.05	78%(3)	74%	5.1%	± 6.5%	4.0°	$\pm 5.0^\circ$
1688	0.49	7.59	50%(4)	47%	4.1%	± 8.5%	5.0°	$\pm 10.4^\circ$
1688	0.68	9.05	50%(4)	47%	-0.5%	± 4.2%	-0.6°	$\pm 5.1^\circ$

(1) from experimental data

(2) theoretical

(3) theoretical, if resonance exists

(4) estimate

1127A9

FIG. 7

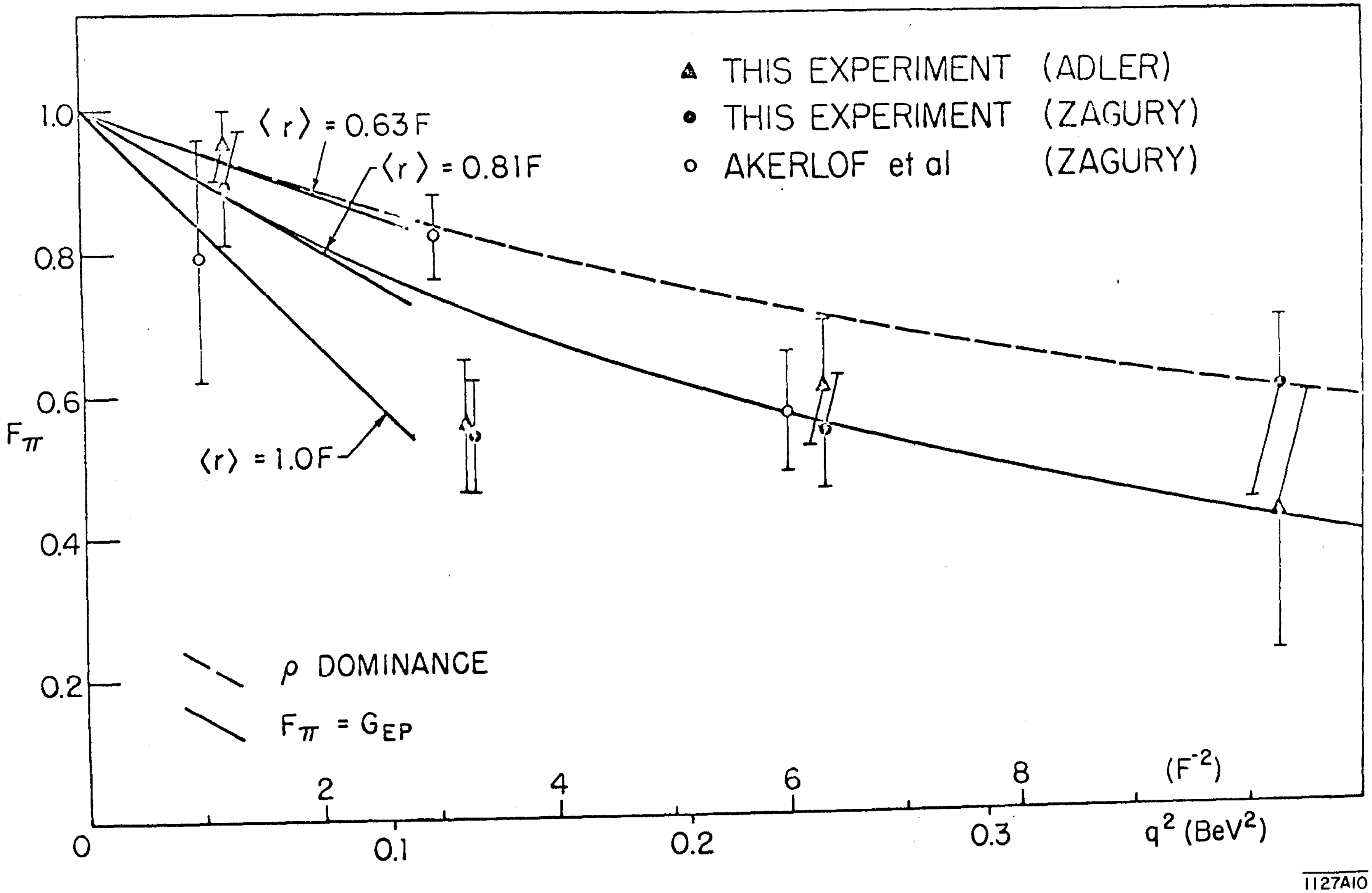

THIS EXPERIMENT (ADLER)
THIS EXPERIMENT (ZAGURY)
AKERLOF et al (ZAGURY)
⟨r⟩ = 0.63F
⟨r⟩ = 0.81F
⟨r⟩ = 1.0F
ρ DOMINANCE
Fπ = GEP
Fπ
1.0
0.8
0.6
0.4
0.2
0
0.1
0.2
0.3
q² (BeV²)
2
4
6
8
(F⁻²)
1127A10

Fig. 8

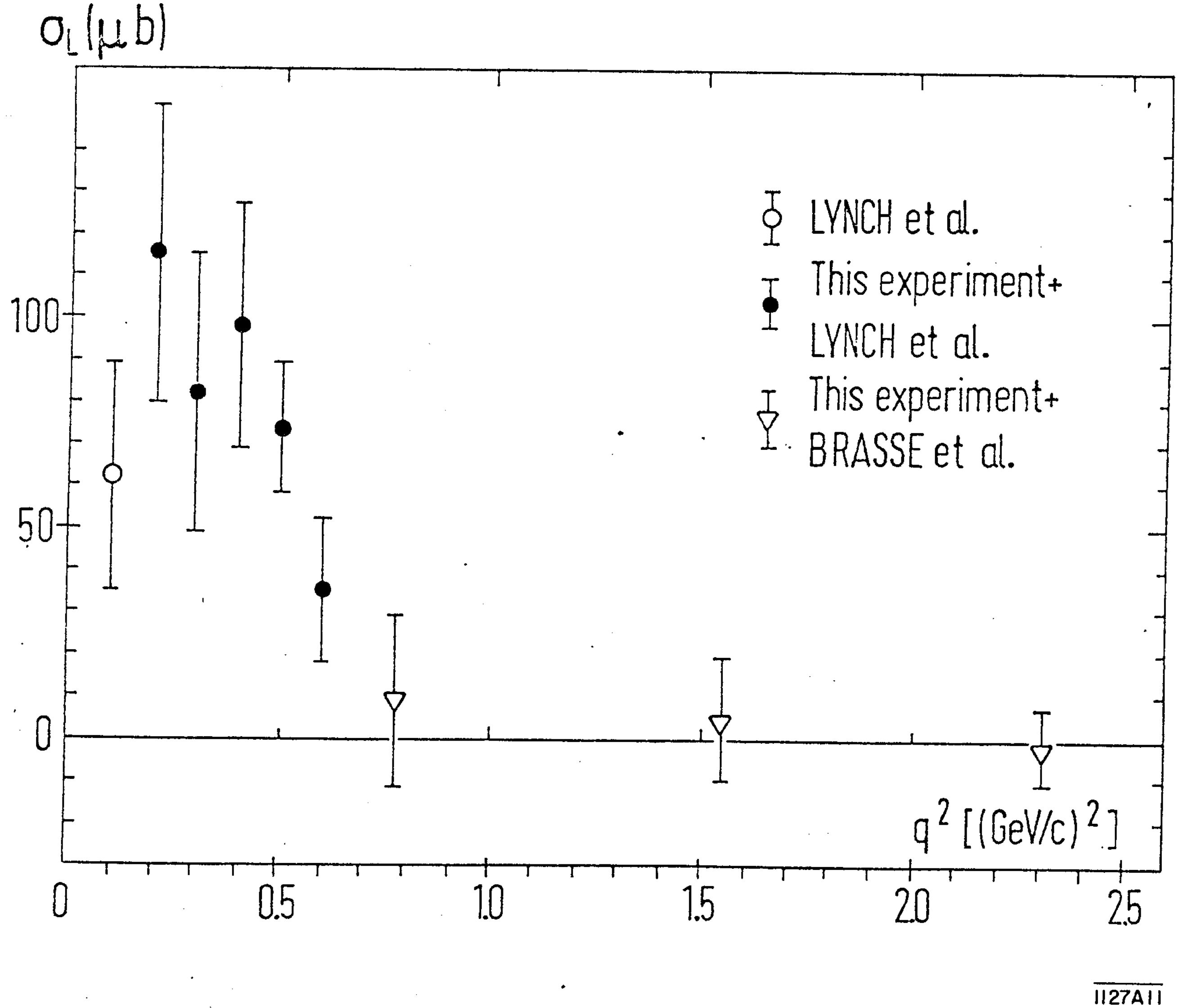

σL (μb)
100
50
0
LYNCH et al.
This experiment+
LYNCH et al.
This experiment+
BRASSE et al.
q2 [(GeV/c)2]
0
0.5
1.0
1.5
2.0
2.5
1127A11

Fig. 9

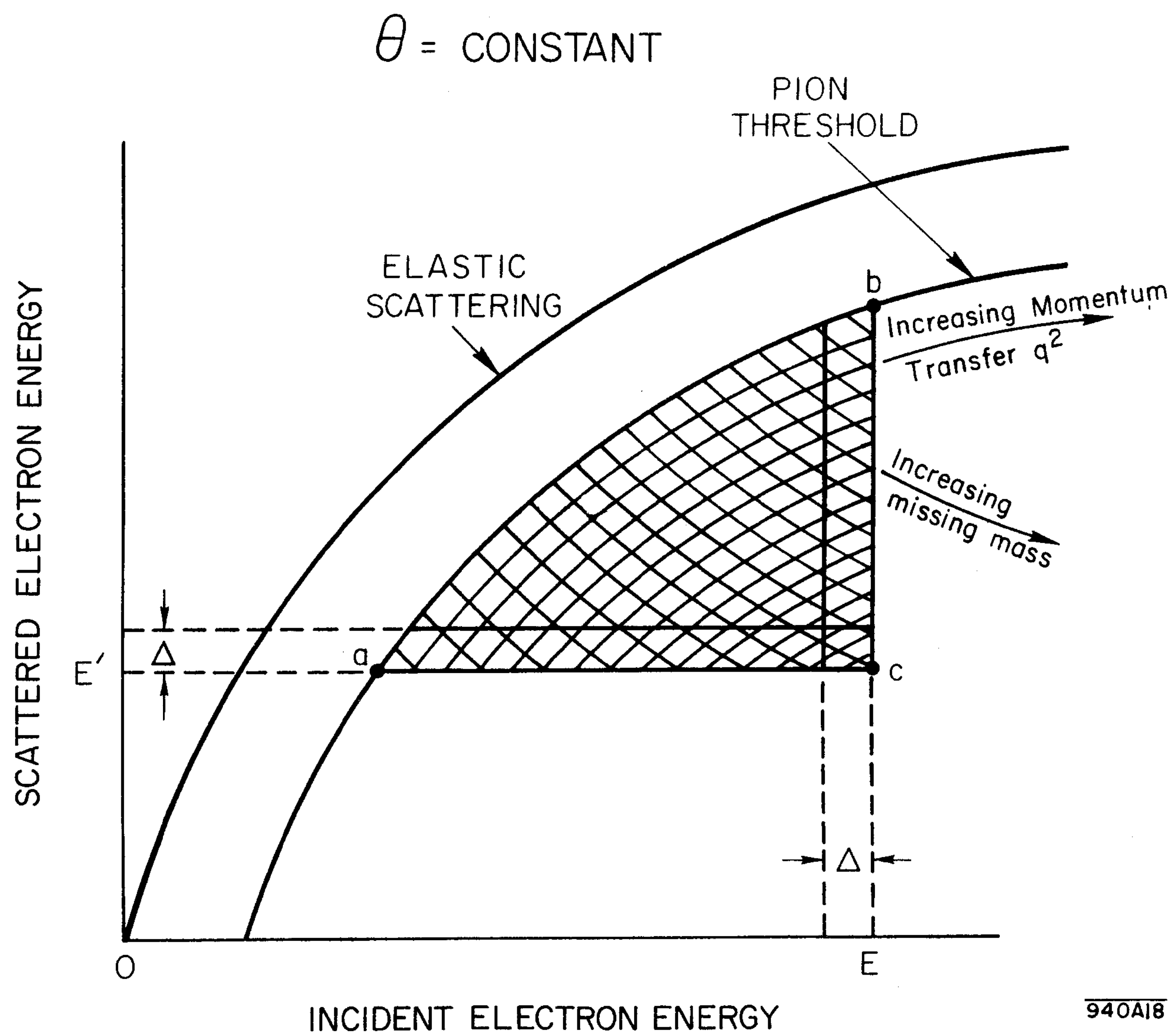
θ = CONSTANT
PION
THRESHOLD
ELASTIC
SCATTERING
b
Increasing Momentum
Transfer q²
Increasing
missing mass
E′
Δ
a
c
Δ
O
E
SCATTERED ELECTRON ENERGY
INCIDENT ELECTRON ENERGY
940A18

Fig. 10

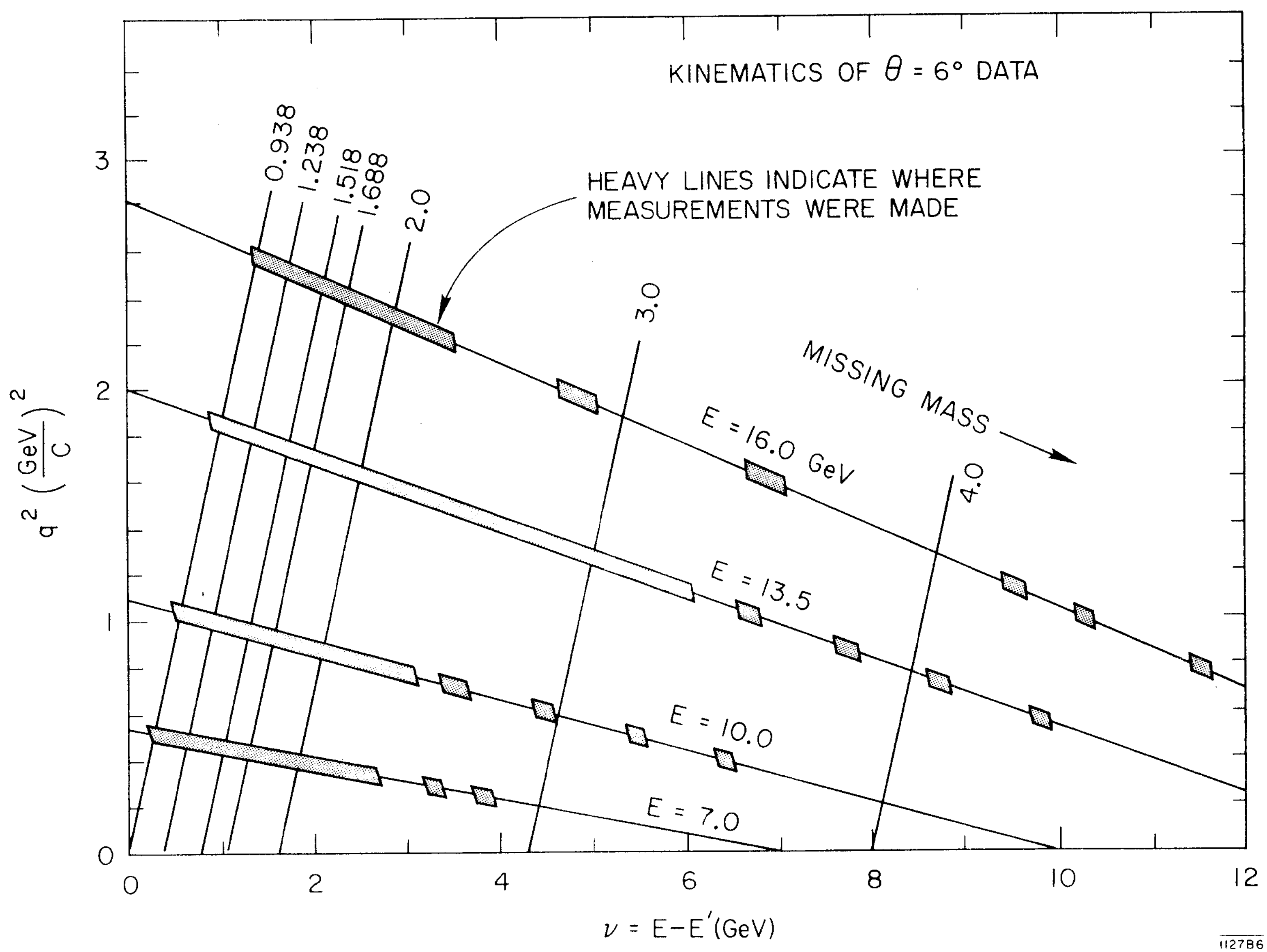
KINEMATICS OF θ = 6° DATA
HEAVY LINES INDICATE WHERE MEASUREMENTS WERE MADE
MISSING MASS
0.938
1.238
1.518
1.688
2.0
3.0
4.0
E = 16.0 GeV
E = 13.5
E = 10.0
E = 7.0
$q^2 \left(\frac{GeV}{c}\right)^2$
ν = E−E′(GeV)
0
1
2
3
0
2
4
6
8
10
12
1127B6

Fig. 11

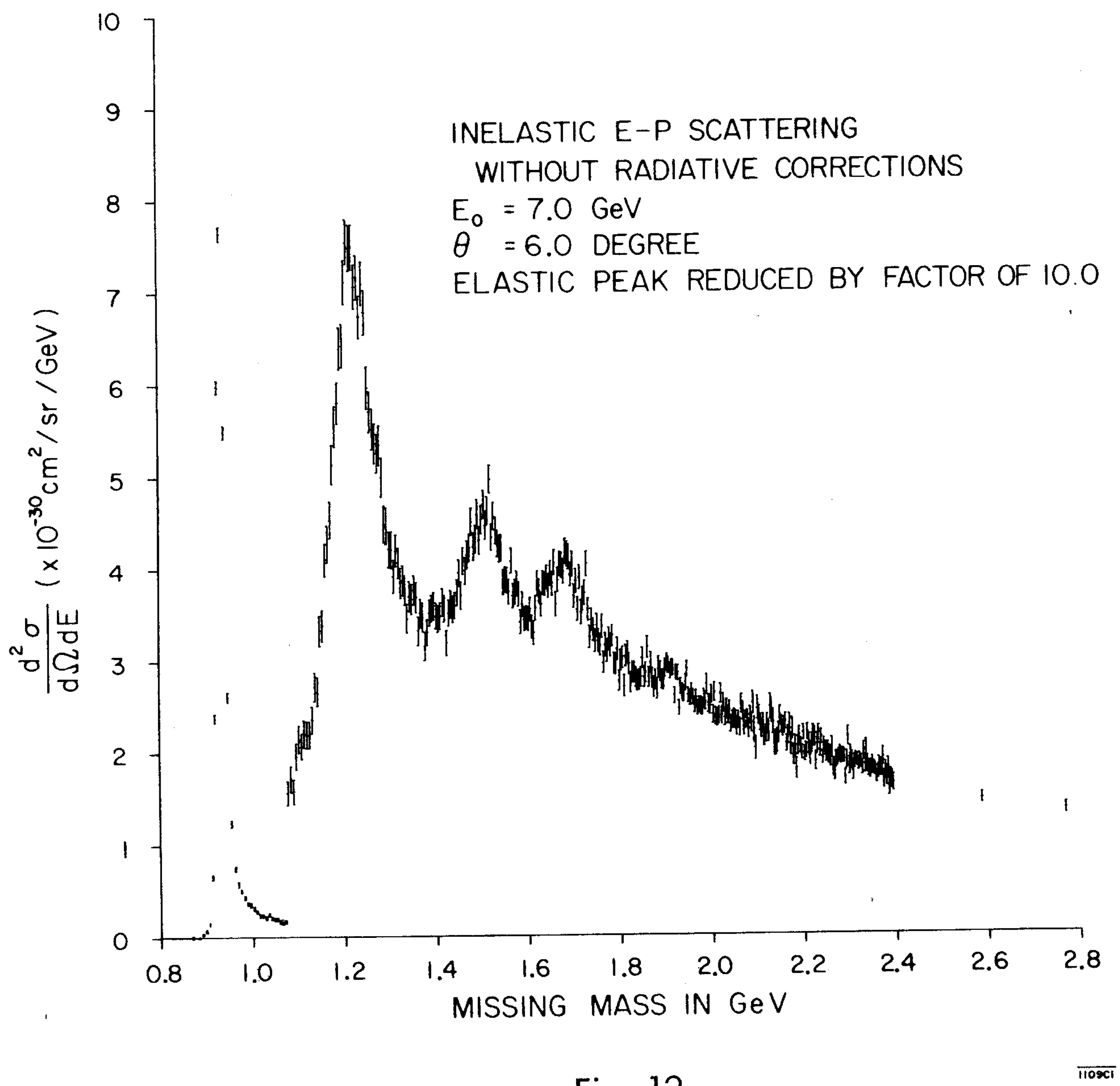
INELASTIC E-P SCATTERING
WITHOUT RADIATIVE CORRECTIONS
E_o = 7.0 GeV
θ = 6.0 DEGREE
ELASTIC PEAK REDUCED BY FACTOR OF 10.0
$\frac{d^2\sigma}{d\Omega dE}$ (x 10^{-30} cm^2/sr/GeV)
MISSING MASS IN GeV
0
1
2
3
4
5
6
7
8
9
10
0.8
1.0
1.2
1.4
1.6
1.8
2.0
2.2
2.4
2.6
2.8
1109C1

Fig. 12

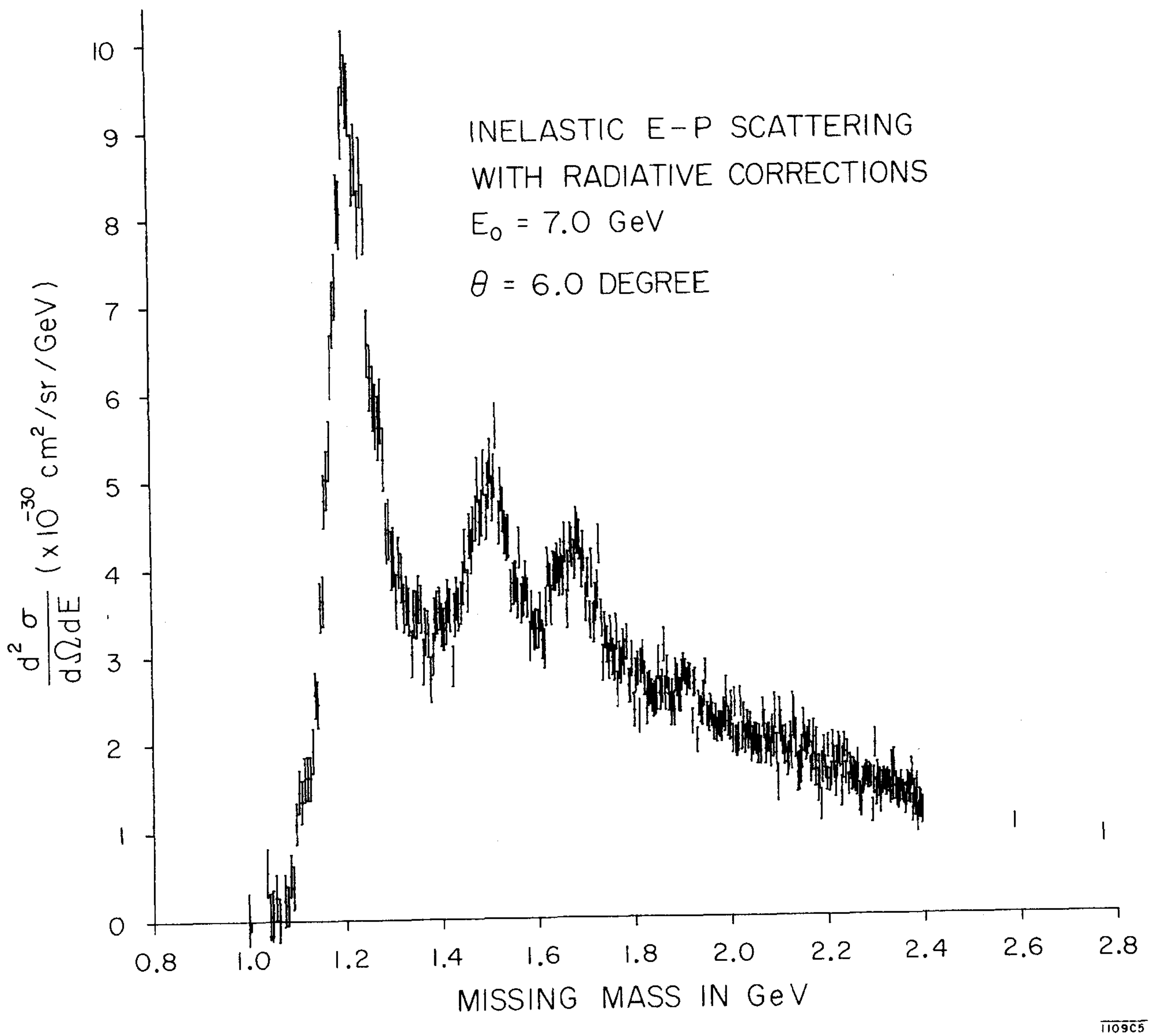
INELASTIC E-P SCATTERING
WITH RADIATIVE CORRECTIONS
E_0 = 7.0 GeV
θ = 6.0 DEGREE
$\frac{d^2\sigma}{d\Omega dE}$ ($\times 10^{-30}$ cm^2/sr/GeV)
MISSING MASS IN GeV
0
1
2
3
4
5
6
7
8
9
10
0.8
1.0
1.2
1.4
1.6
1.8
2.0
2.2
2.4
2.6
2.8
1109C5

Fig. 13

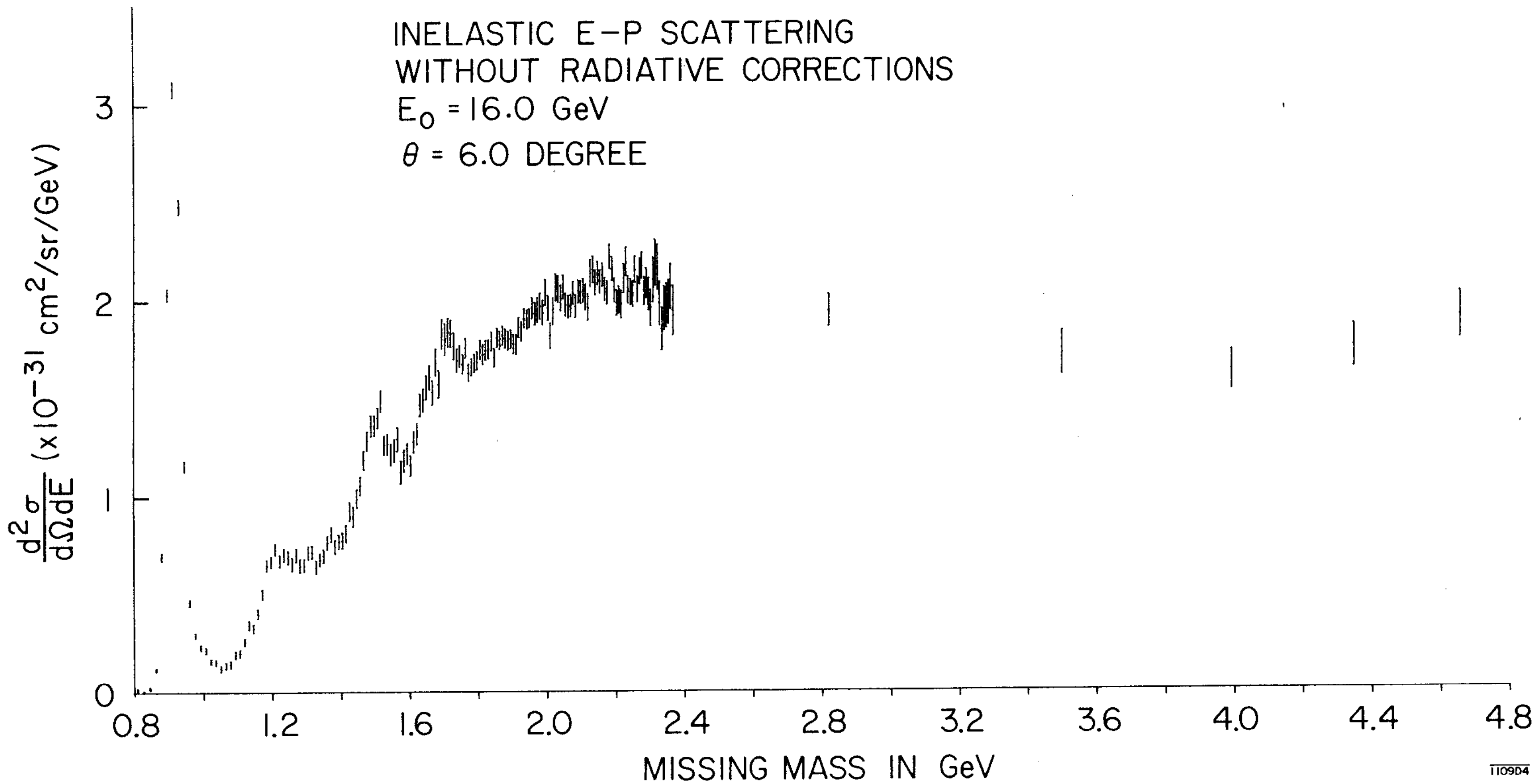
INELASTIC E-P SCATTERING
WITHOUT RADIATIVE CORRECTIONS
E0 = 16.0 GeV
θ = 6.0 DEGREE
d²σ/dΩdE (x10⁻³¹ cm²/sr/GeV)
0
1
2
3
0.8
1.2
1.6
2.0
2.4
2.8
3.2
3.6
4.0
4.4
4.8
MISSING MASS IN GeV
1109D4

Fig. 14

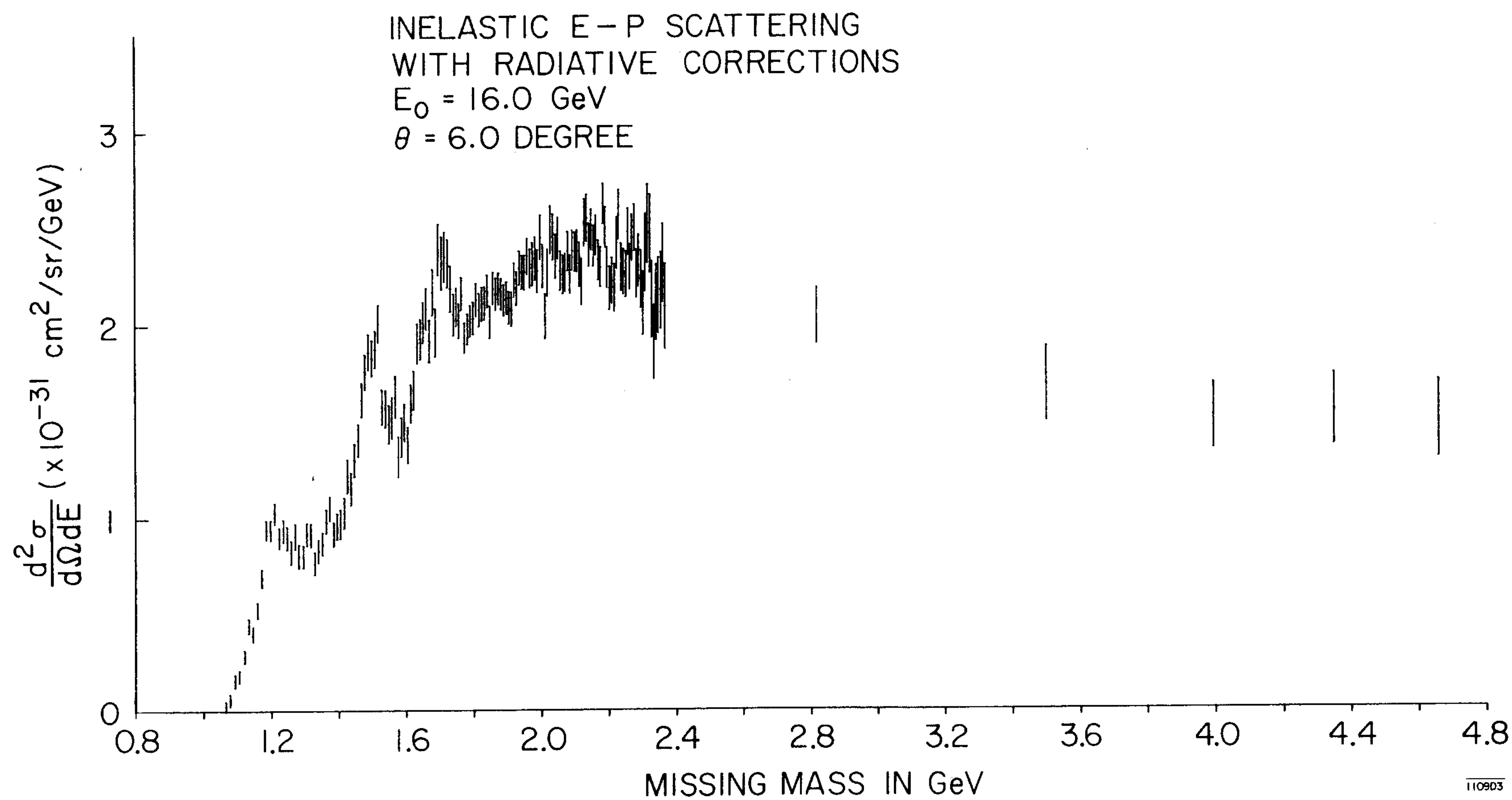

INELASTIC E-P SCATTERING
WITH RADIATIVE CORRECTIONS
E_0 = 16.0 GeV
θ = 6.0 DEGREE
$\frac{d^2\sigma}{d\Omega dE}$ ($\times 10^{-31}$ cm^2/sr/GeV)
0
1
2
3
0.8
1.2
1.6
2.0
2.4
2.8
3.2
3.6
4.0
4.4
4.8
MISSING MASS IN GeV
1109D3

Fig. 15

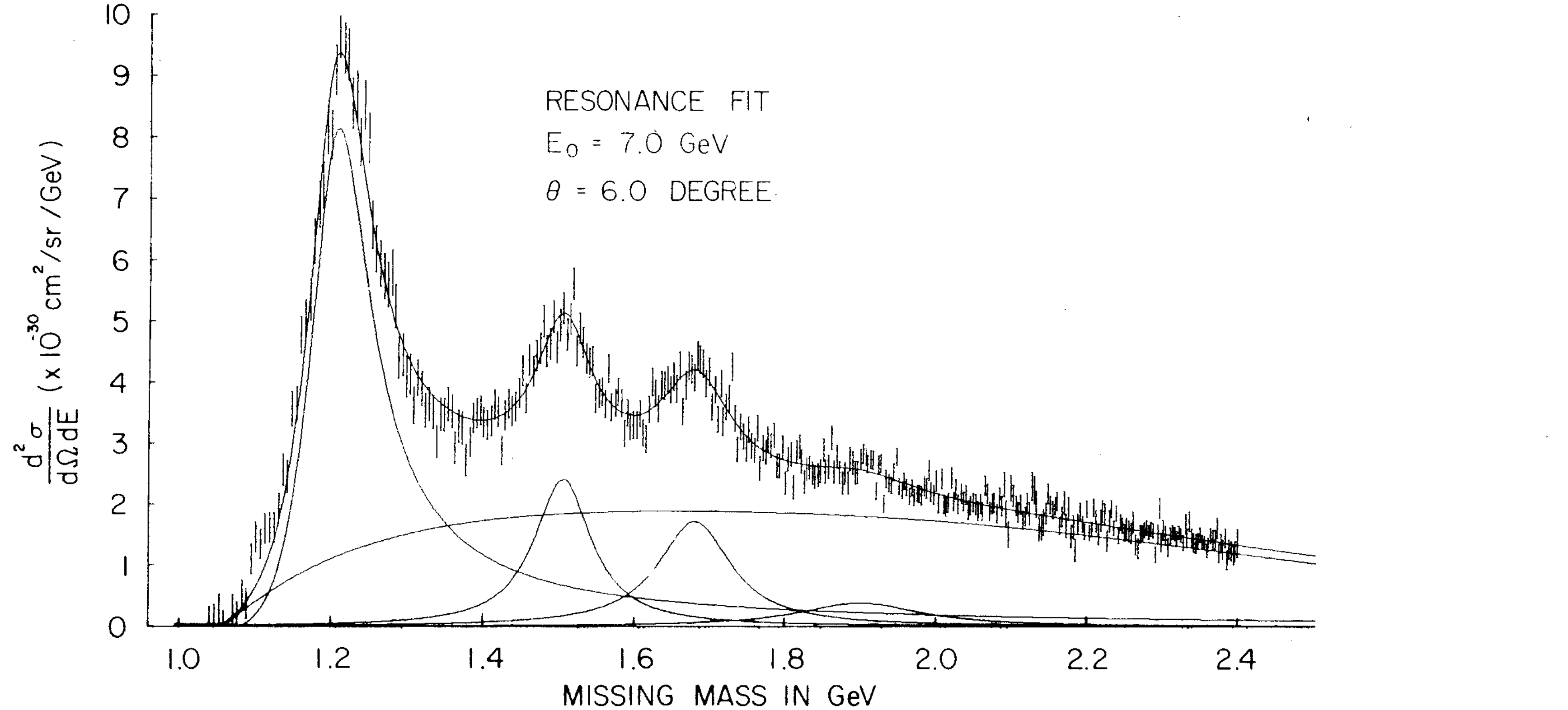

RESONANCE FIT
E_0 = 7.0 GeV
θ = 6.0 DEGREE
$\frac{d^2\sigma}{d\Omega dE}$ (x 10^{-30} cm^2/sr /GeV)
MISSING MASS IN GeV
0
1
2
3
4
5
6
7
8
9
10
1.0
1.2
1.4
1.6
1.8
2.0
2.2
2.4
110906

Fig. 16

E_0 (GeV)	θ_0 (Degree)	$\frac{d\sigma}{d\Omega}$ (cm^2/sr)		
		N_1^* M = 1.219 ± 0.010 GeV Γ = 0.130 GeV	N_2^* M = 1.503 ± 0.010 GeV Γ = 0.077 GeV	N_3^* M = 1.691 ± 0.010 GeV Γ = 0.102 GeV
7.00	6.000	$(2.15 \pm 0.17) \times 10^{-30}$	$(5.21 \pm 0.37) \times 10^{-31}$	$(5.30 \pm 0.29) \times 10^{-31}$
10.00	6.000	$(3.95 \pm 0.25) \times 10^{-31}$	$(1.36 \pm 0.12) \times 10^{-31}$	$(1.48 \pm 0.16) \times 10^{-31}$
13.50	6.000	$(7.02 \pm 0.84) \times 10^{-32}$	$(3.62 \pm 0.40) \times 10^{-32}$	$(4.17 \pm 0.83) \times 10^{-32}$
16.02	6.000	$(1.24 \pm 0.19) \times 10^{-32}$	$(9.81 \pm 1.41) \times 10^{-33}$	$(1.43 \pm 0.42) \times 10^{-32}$

1127A12

Fig. 17

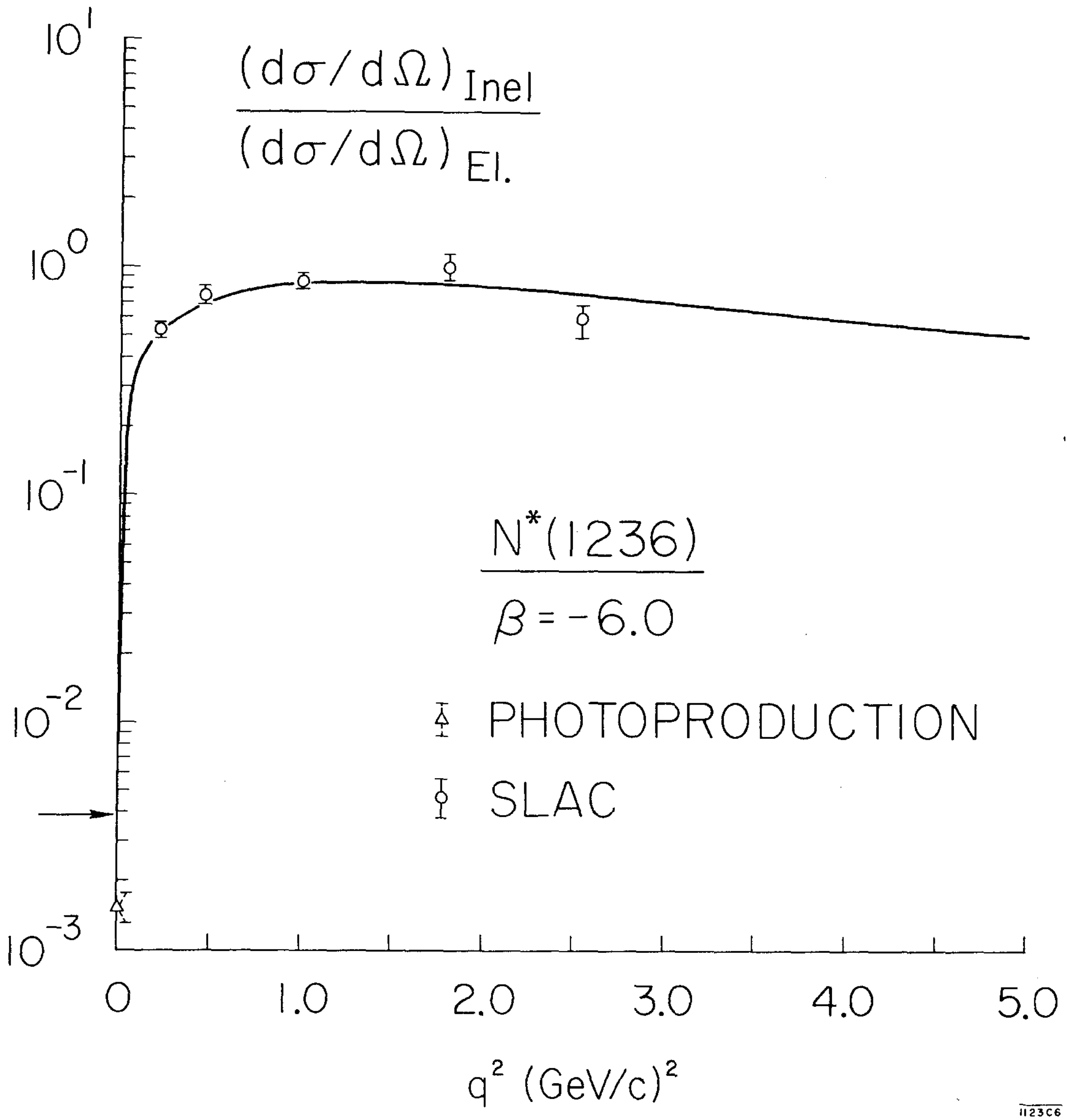

$\frac{(d\sigma/d\Omega)_{Inel}}{(d\sigma/d\Omega)_{El.}}$
N*(1236)
β = -6.0
PHOTOPRODUCTION
SLAC
10^1
10^0
10^-1
10^-2
10^-3
0
1.0
2.0
3.0
4.0
5.0
q^2 (GeV/c)^2
1123C6

Fig. 18

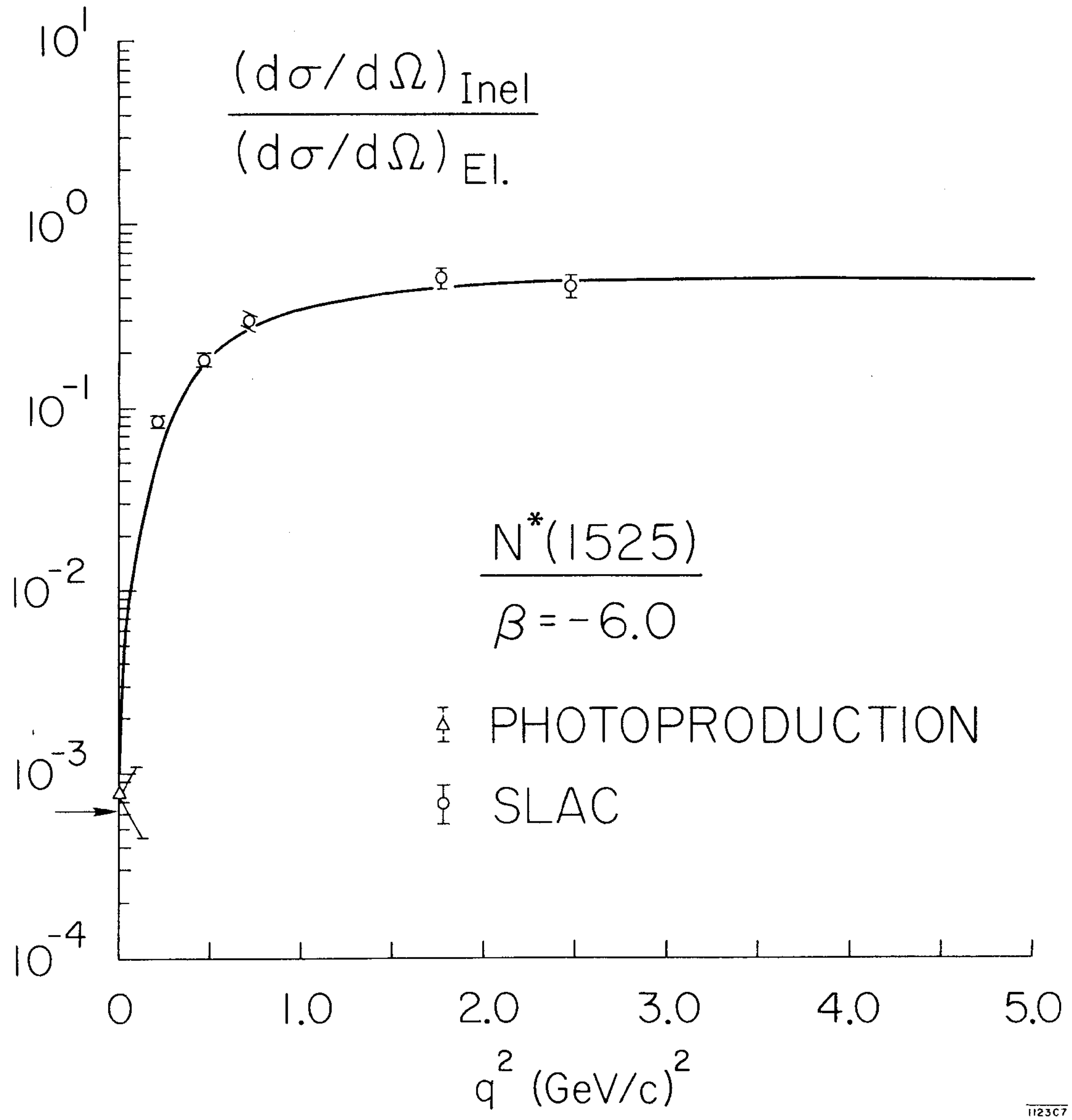

$\frac{(d\sigma/d\Omega)_{Inel}}{(d\sigma/d\Omega)_{El.}}$
10^1
10^0
10^{-1}
10^{-2}
10^{-3}
10^{-4}
$N^*(1525)$
$\beta = -6.0$
PHOTOPRODUCTION
SLAC
0
1.0
2.0
3.0
4.0
5.0
q^2 $(GeV/c)^2$
1123C7

Fig. 19

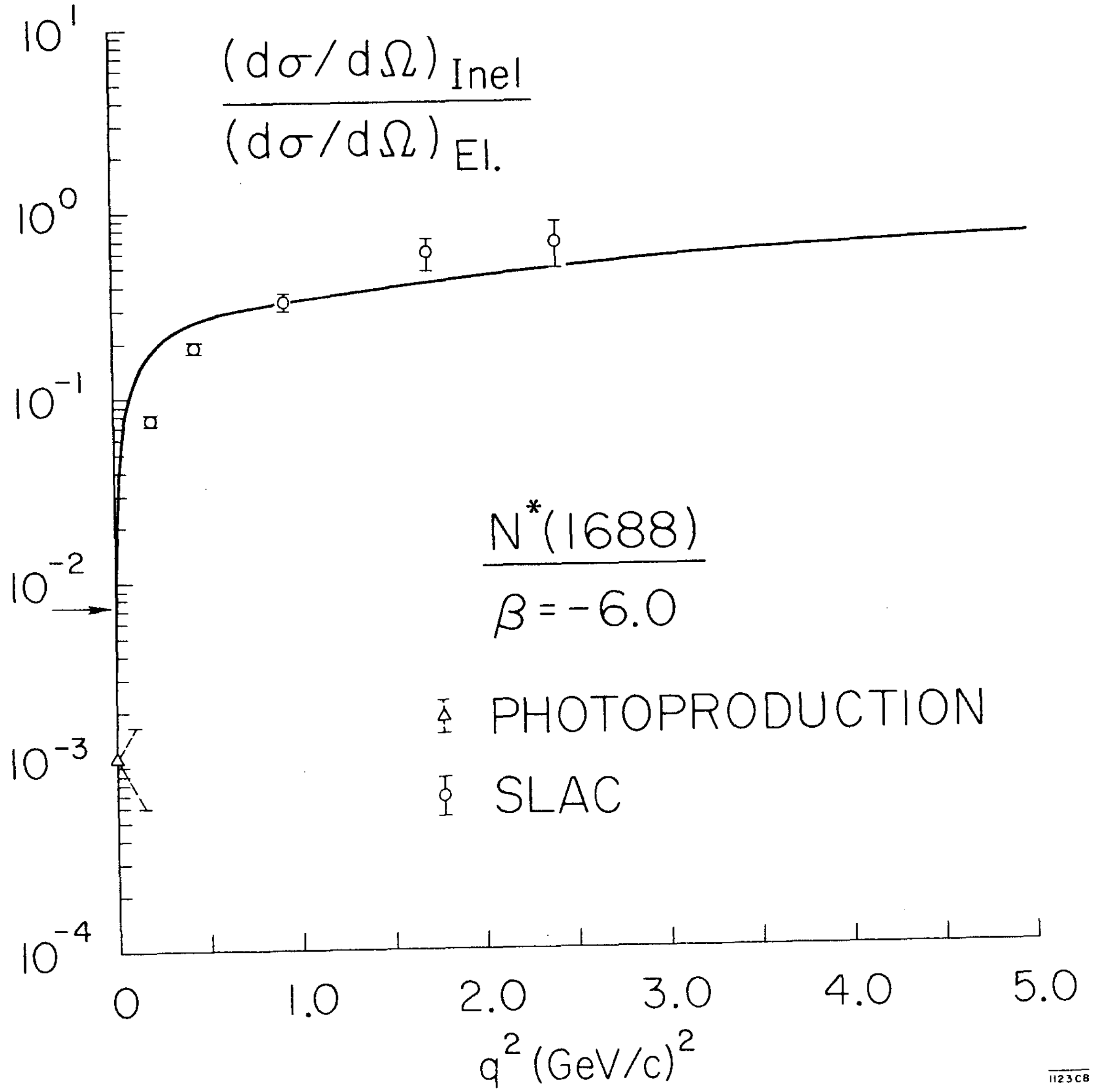

10^1
10^0
10^{-1}
10^{-2}
10^{-3}
10^{-4}
$\frac{(d\sigma/d\Omega)_{Inel}}{(d\sigma/d\Omega)_{El.}}$
$N^*(1688)$
$\beta = -6.0$
PHOTOPRODUCTION
SLAC
0
1.0
2.0
3.0
4.0
5.0
q^2 (GeV/c)^2
1123C8

Fig. 20

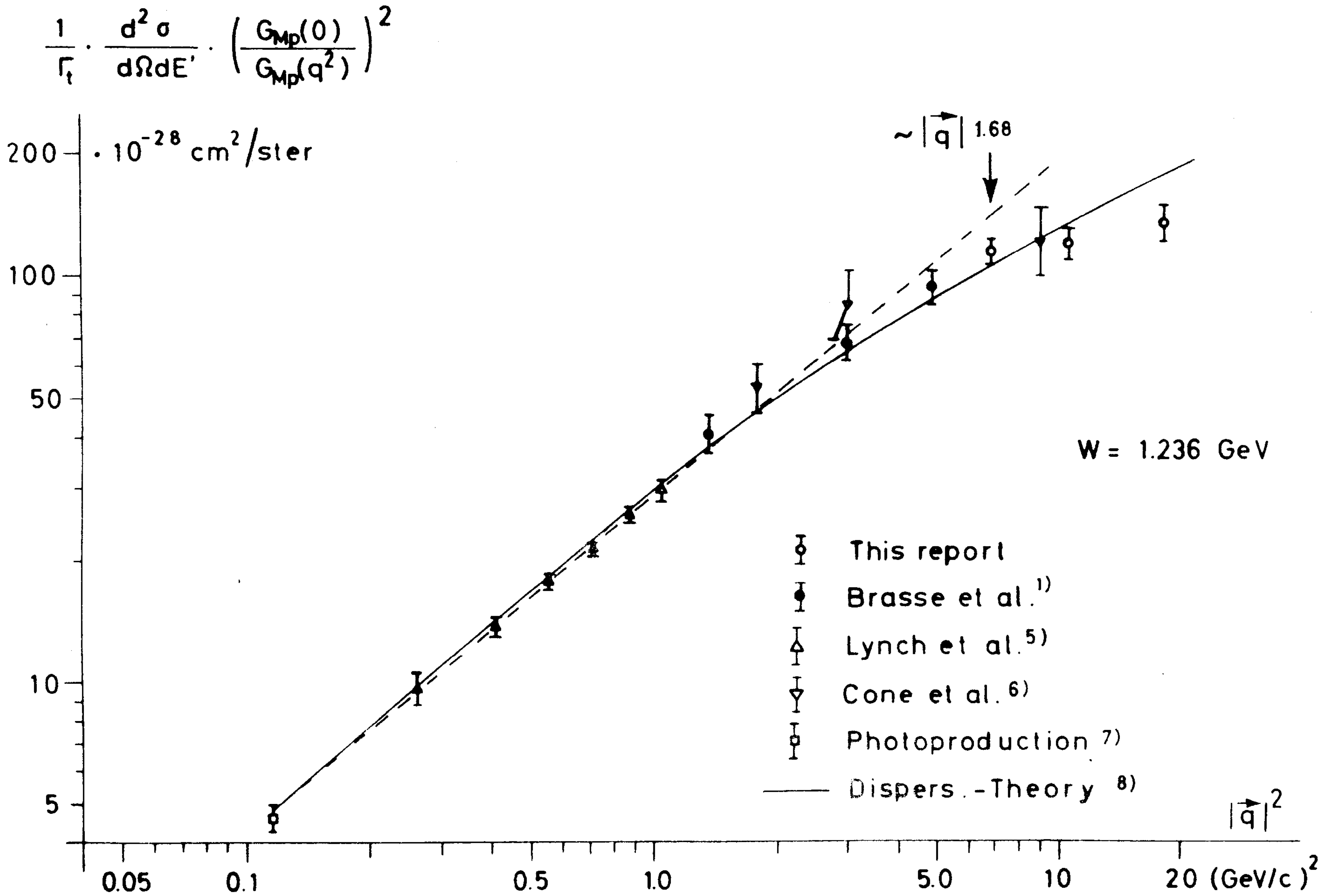

1127A13

Fig. 21

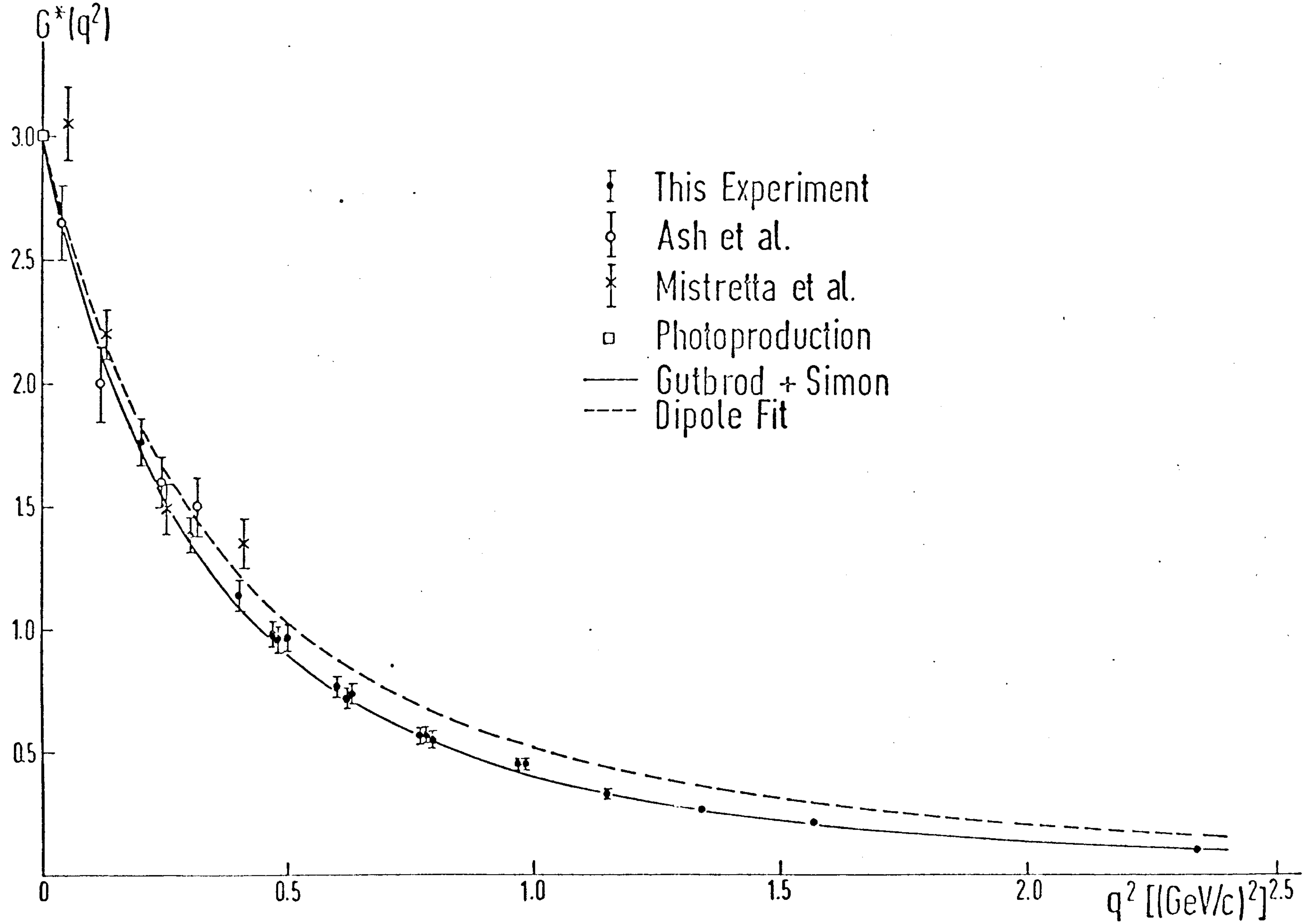

Fig. 22

1127A14

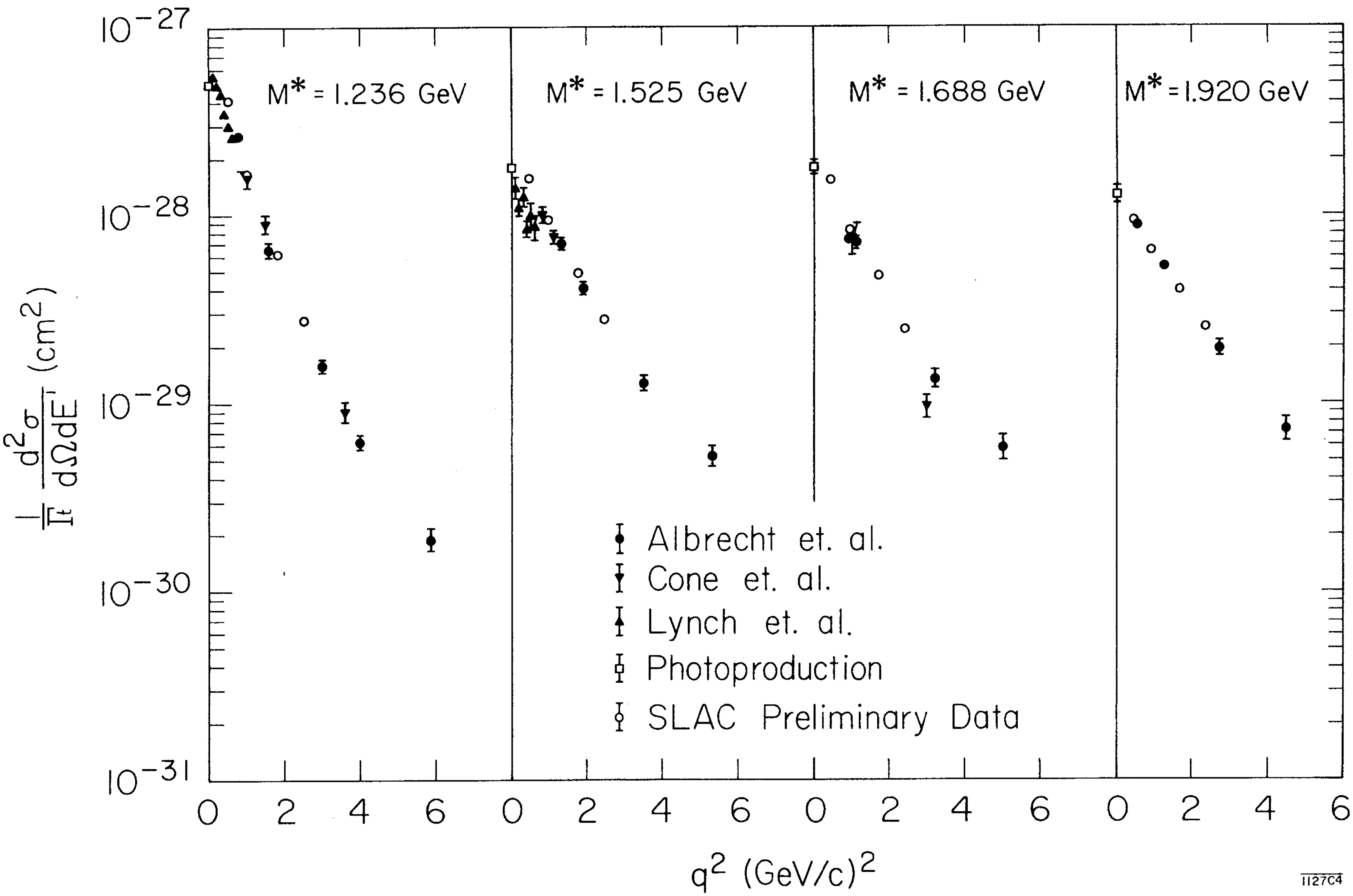

10^{-27}
10^{-28}
10^{-29}
10^{-30}
10^{-31}
$\frac{1}{\Gamma_t}\frac{d^2\sigma}{d\Omega dE'}$ (cm^2)
M* = 1.236 GeV
M* = 1.525 GeV
M* = 1.688 GeV
M* = 1.920 GeV
Albrecht et. al.
Cone et. al.
Lynch et. al.
Photoproduction
SLAC Preliminary Data
0 2 4 6 0 2 4 6 0 2 4 6 0 2 4 6
q^2 (GeV/c)^2
1127C4

Fig. 23

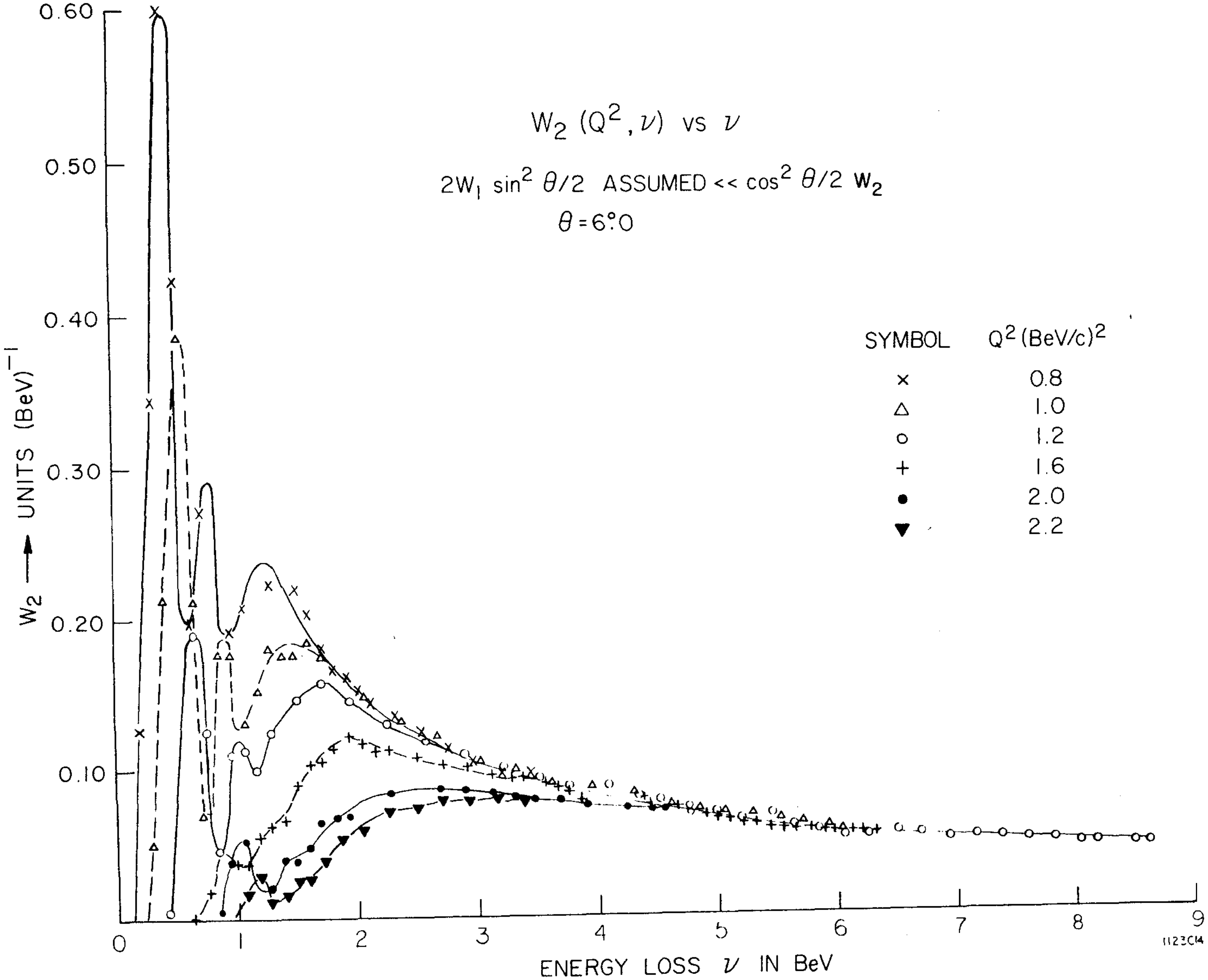

W2 (Q2, ν) vs ν
2W1 sin2 θ/2 ASSUMED << cos2 θ/2 W2
θ = 6.0°
SYMBOL Q2 (BeV/c)2
× 0.8
△ 1.0
○ 1.2
+ 1.6
● 2.0
▼ 2.2
W2 ⟶ UNITS (BeV)−1
0.60
0.50
0.40
0.30
0.20
0.10
0
1
2
3
4
5
6
7
8
9
ENERGY LOSS ν IN BeV
1123C14

Fig. 24

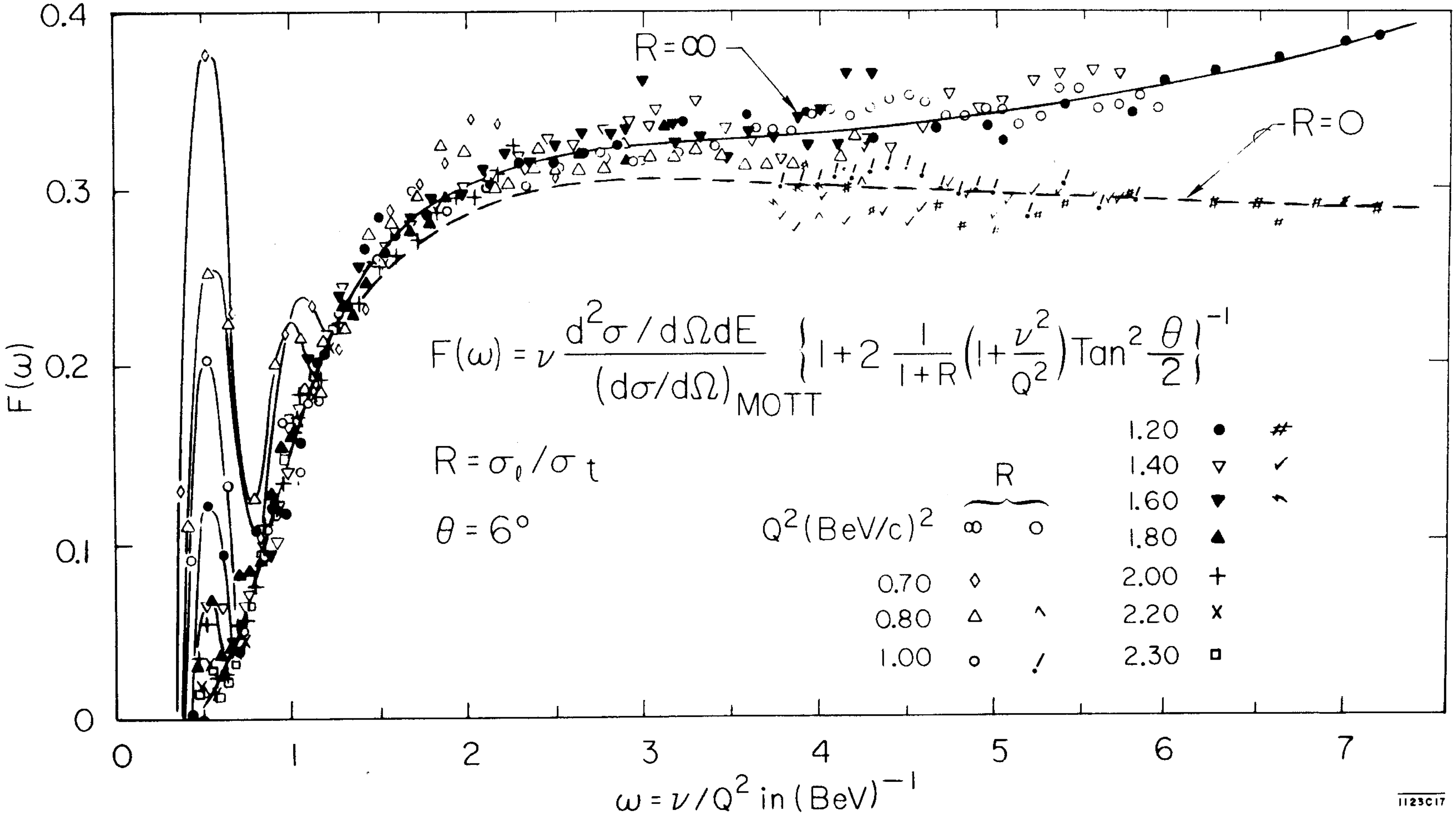

0.4
0.3
0.2
0.1
0
F(ω)
0
1
2
3
4
5
6
7
ω = ν/Q² in (BeV)⁻¹
R = ∞
R = 0
F(ω) = ν (d²σ/dΩdE)/(dσ/dΩ)_MOTT {1 + 2 (1/(1+R)) (1 + ν²/Q²) Tan² θ/2}⁻¹
R = σ_ℓ/σ_t
θ = 6°
R
Q²(BeV/c)²
∞
0
0.70
0.80
1.00
1.20
1.40
1.60
1.80
2.00
2.20
2.30
1123C17

Fig. 25